Binding Energies in Atomic Negative Ions: III[a)]

T. Andersen[b)]
Institute of Physics and Astronomy, University of Aarhus, DK-8000 Aarhus C, Denmark

H. K. Haugen[c)]
Department of Physics and Astronomy, McMaster University, Hamilton, Ontario L8S4M1, Canada

H. Hotop[d)]
Fachbereich Physik, Universität Kaiserslautern, D-67653 Kaiserslautern, Germany

Received July 9, 1999; revised manuscript received October 5, 1999

This article updates a 14 yr old review on this subject [J. Phys. Chem. Ref. Data **14**, 731 (1985)]. A survey of the electron affinity determinations for the elements up to $Z=94$ is presented, and based upon these data, a set of recommended electron affinities is established. New developments in the experimental methods which yield accurate electron binding energies are described. Fine structure splittings and excited state energies of negative ions as well as lifetimes of metastable states are given. Progress in theoretical calculations of atomic electron affinities is documented by comparison with reliable experimental data. © *1999 American Institute of Physics and American Chemical Society.* [S0047-2689(99)00206-8]

Key words: ab initio calculations; atomic negative ions; binding energy; electron affinity; excited states; experimental methods; fine structure splitting; recommended values; semiempirical calculations; metastable states; lifetimes.

Contents

[a)]Dedicated to Professor W. Carl Lineberger on the occasion of his 60th birthday.

[b)]Electronic mail: fystor@ifa.au.dk
[c)]Electronic mail: haugenh@mcmaster.ca
[d)]Electronic mail: hotop@physik.uni-kl.de

List of Tables

List of Figures

1. Introduction

Fourteen years have passed since Hotop and Lineberger [HL85] reviewed and compiled the knowledge of binding energies in atomic negative ions. Since that time, several survey articles have dealt with this subject in a more or less selective way [Ba91, B195, AAB97, An97]. The physics of short-lived resonance states of atomic negative ions has been addressed in a recent comprehensive review [BC94].

Since the publication of the 1985 review [HL85] some interesting developments, both experimental and theoretical, have deepened our insight into the physics of atomic negative ions. The existence of bound states of the alkaline earth atomic negative ions was firmly established in parallel experimental and theoretical work in 1987 [FLV87, PTC87, Pe92], and new methods including threshold photodetachment to excited states of the neutral atom in conjunction with resonance ionization detection of the latter have allowed unambiguous and precise determinations of binding energies in weakly bound atomic negative ions [electron affinity (EA)$<$0.2 eV] [PVB95, AAB97]. The use of narrow-band, coherent radiation for detailed investigations of photodetachment thresholds in the ultraviolet and infrared range has resulted in much improved values of the binding energies for ground and excited states in several important atomic negative ions, see, e.g., [BCD89, HG92, BGH95, SHB97, SBB98b, SBH98b]. Resonant multiphoton detachment and stimulated Raman scattering detachment spectroscopy have yielded accurate values for fine structure splittings and excited state binding energies. New information on metastable states of atomic negative ions has been obtained over the la 8 yrs with the use of ion storage rings. Accelerator ma spectrometry has helped in establishing the stability of se eral hitherto undetected atomic negative ions.

On the theory side, substantial progress has been made i the accurate *ab initio* description of the negative ions wi atomic number $Z=3-5$, including estimates of the remai ing uncertainty in the resulting binding energies. Progre has also been substantial, however, for atoms of higher Z The theoretical approaches include, e.g., multiconfiguratic Hartree–Fock (MCHF) with relativistic correctio [FYG95], multiconfiguration Dirac–Fock (MCDF) [Wi97 relativistic coupled-cluster (RCC) [EIP97], multiferenc configuration interaction (MR-CI), [AMN92] a (r_{12})-MR-CI [Gd99]. An especially important and critic aspect in the calculations is the proper inclusion of core p larization and core rearrangement, especially for weak bound systems.

In view of all these interesting developments and the r sulting increased knowledge, we consider it justified to pr vide a new critical evaluation of binding energies in atom negative ions. In the spirit of the 1985 review, we shall i clude descriptions of some of the basic methods for negati ion spectroscopy with emphasis on the new techniques. W mainly discuss experimental aspects, but we also addre theoretical results to illustrate the recent progress and prese status, e.g., in Sec. 2 where we survey the electron affiniti for atoms with $Z=1-5$. In Sec. 3, we introduce basic aspec of laser photodetachment spectroscopies on which most the known binding energies in atomic negative ions rel New developments in negative ion spectroscopy will be di cussed in six subsections in Sec. 4. In Sec. 5 we surv recent experimental determinations of atomic EAs, includi theoretical results for comparison in selected cases. In Sec 6, 7, and 8 we provide listings of recommended values f binding energies, fine structure splittings, and lifetimes long-lived excited states in atomic negative ions. We co clude with an outlook on future perspectives of this field.

2. Calculation of Electron Affinities

The EA of an atom A is defined as the difference betwe the total energies (E_{tot}) of the ground state of A and negative ion A^-:

$$EA(A)=E_{tot}(A)-E_{tot}(A^-). \quad (2.$$

By ground state, one refers to the lowest energy hyperfin structure level of A and A^-, respectively. The quanti EA(A) is positive for stable negative ions A^-. The total e ergy can be written as

$$E_{tot}=E_{HF}+E_c+E_{so}+\delta. \quad (2.$$

E_{HF} corresponds to the (restricted) Hartree–Fock energy, E_c is the nonrelativistic correlation energy describing the devi tion of the many-electron system from the Hartree–Fo (HF) self-consistent-field (SCF) model, E_{so} is the spin-orb energy for states with nonzero orbital angular momentu and spin, and δ comprises correction terms including hyp

TABLE 1. Comparison between theoretical and experimental binding energies for negative ions with $Z=1-5$

Z	Atom	Atomic State	Neg. Ion State	BE $(cm^{-1})_{THEO.}$	BE $(cm^{-1})_{EXP.}$	Ref.$_{THEO.}$	Ref.$_{EXP.}$
1	H	$1s\,^2S_{1/2}(F=0)$	$1s^2\,^1S_0$	6083.064 145 (30)	6082.99(15)	Dr99	LML91
2	He	$1s2s\,^3S_1$	$1s2s2p\,^4P_{5/2}$	625.27(3)	625.21(5)	YC99	KPP97
3	Li	$2s\,^2S_{1/2}$	$2s^2\,^1S_0$	4981.6(9)	4984.90(17)	Fi93	HHK96
4	Be	$2s2p\,^3P_0$	$2s2p^2\,^4P_{3/2}$	2330(8)	2344.9(8)	HC95	KPA95
5	B	$2p\,^2P_{1/2}$	$2p^2\,^3P_0$	2250(16)	2256.12(20)	FYG95	SHB98b

fine structure, mass polarization, and radiative effects (Lamb shift). Electron correlation effects are decisive for the stability in many atomic negative ions [HL75] which therefore represent a sensitive testing ground for many-electron theories.

The best known electron affinity is that of the hydrogen atom, as obtained in elaborate numerical calculations [Pe62, Dr88, Dr99] with uncertainities below 0.001 cm^{-1} ($\approx 10^{-7}$ eV, 1 eV=8065.544 77(32) cm^{-1} [Ta99]). The most accurate results, including improved values for the relativistic recoil and the QED correction terms, have been recently obtained by Drake (see also [DM98]). The nonrelativistic binding energy of H^- amounts to 6087.328 861 cm^{-1} [Dr99] (for infinite nuclear mass). With first and second order mass polarization this value changes to 6083.406 916 cm^{-1}; including relativistic corrections one obtains 6083.102 684 cm^{-1}. With incorporation of relativistic recoil, Lamb shift and nuclear recoil corrections, the H^- binding energy (omitting hyperfine structure) is calculated as 6083.099 68(3) cm^{-1} [Dr99], where the error bar stems mainly from the uncertainty of the QED terms [Dr99]. Finally, using the accurately known $F=0-1$ hyperfine interval in H($1s$) of 0.047 379 635 94 cm^{-1} [CKR63], the EA of the hydrogen atom is obtained as EA[H($1s, F=0$)] = 6083.064 145(30) cm^{-1} (relative uncertainty $5\cdot 10^{-9}$).

Substantial progress has been recently made in the accurate theoretical determination of EAs for the light elements (up to $Z=5$) and of the energies and photodetachment spectra involving (doubly) excited states of negative ions.

Table 1 illustrates the progress obtained since 1985 [HL85] with respect to the accuracy of experimentally determined binding energies (a factor of 10–100), but the reliability of the predicted values has also been improved quite considerably. For H^- theory is ahead of experiment, whereas the experimental value for He^-, obtained with laser photodetachment threshold (LPT) combined with resonance ionization spectroscopy [KPP97] (see Sec. 4.2) can challenge the most accurate theoretical result. Table 1 indicates the difficulties the theoretical calculations have to deal with when the number of electrons increases, resulting in less accurate predictions, but the overall agreement with the experimental values is impressive.

The study of the binding energy of the Be^- ion can illustrate the progress obtained since the 1985 review. The binding energy for the $2s2p^2\,^4P$ state was first measured that year by Kvale *et al.* [KAC85] to be 190(90) meV by autodetachment electron spectroscopy. In 1993 Tang *et al.* [TWP93] applied laser photodetached electron spectroscopy (LPES) and obtained 261(10) meV. At that time the best theoretical estimate yielded 276.1(6.5) meV [Bu86], so the experimental and theoretical values were considered to be in agreement within the error bars quoted. Subsequently, however, Olsen *et al.* [OPS94] and Hsu and Chung [HC95] performed very elaborate calculations, with careful treatment of the core–core and core–valence effects, yielding a larger binding energy, 285(5) meV and 288.9(1.0) meV (or 2330(8) cm^{-1}), respectively. These predictions clearly deviated from the experimental value of Tang *et al.* [TWP93] and prompted a reinvestigation of the binding energy of Be^- using LPT combined with resonance ionization spectroscopy. The experimental binding energy for the $^4P_{3/2}$ state was now measured to be 290.74(10) meV or 2344.9(8) cm^{-1} [KPA95], in good agreement with the most recent theoretical result (deviation less than 1%). This difference might be reduced taking into consideration some small contributions to the theoretical value, which so far have been neglected [Ch97]. It should be noted that the theoretical data given for Be and B were published ahead of the experimental results, indicating a significant success for the computational methods used.

Studies of heavier negative ions have shown [SWL96, HLH93, PAA98] that computational methods, such as many-body perturbation calculations, now are able to predict the binding energy of negative ions such as Ca^- ($Z=20$) within 15–40 cm^{-1}, when third order correction terms are taken into account. For still heavier systems like $Z=70$ (Yb^-), the calculations have yielded predictions with an estimated accuracy of 100–150 cm^{-1} [AB97].

The significantly improved quality of the many-body perturbation calculations has made the predicted binding energies very valuable, particularly for ions for which no experimental data are available. The predicted values are far better than semiempirical values obtained by extrapolations along homologous sequences.

3. Principles of Negative Ion Spectroscopy

3.1. Introductory Remarks

The aim of negative ion spectroscopy in the context of the present review is the accurate determination of binding energies in the negative ions under study. In contrast to neutral

atoms and positive ions, no Rydberg series exist in negative ions for which the long-range attractive interactions $V(r)$ between the electron and the atom A decrease rapidly, i.e., at large electron–atom distances r, $V(r) \sim r^{-m}$, with $m > 2$. Consequently, binding energies have to be determined by measurements of a suitable bound-free photodetachment transition, induced by photons γ of defined energy $E_\gamma = h\nu$

$$A^-(i) + \gamma \rightarrow A(f) + e^-(\varepsilon_{if\gamma}). \quad (3.1)$$

In the rest frame of the ion the energy of the photoelectron for the detachment channel $i \rightarrow f$ is given by

$$\varepsilon_{if\gamma} = E_\gamma - (E_f - E_i). \quad (3.2)$$

Equation (3.2) forms the basis for the determination of binding energies by photodetachment electron spectrometry (PES) (Sec. 3.4). PES is a versatile method, but its energy resolution has been typically in the range of 10–30 meV and in a few cases 3–5 meV [HL85]. Much more accurate determinations of binding energies can be achieved by measurements of the threshold photon energy

$$E_{\mathrm{THR},if} = h\nu_{\mathrm{THR},if} = E_f - E_i \quad (3.3)$$

at which the channel $i \rightarrow f$ opens (Sec. 3.3.). Using tunable narrow band lasers (or laser-based coherent light sources), LPT spectroscopy represents the method of choice for measuring electron affinities and binding energies of excited negative ions. In Sec. 3.2., we briefly dwell on some important experimental aspects of negative ion spectroscopy.

3.2. Experimental Aspects

Photodetachment studies require: (i) a well-characterized sample of negative ions, (ii) a sufficiently intense, narrow band source of photons, and (iii) a suitable detector for the products of reaction (3.1).

(i) Atomic negative ions are produced in discharge or sputter ion sources and by (double)-electron capture of a beam of positive ions A^+ traversing a suitable target gas. Sputter ion sources, involving bombardment of metal cathodes by Cs^+ ions, are well suited for the production of intense negative ion beams of essentially all metals [Mi83, Mi89]. Fragile, weakly bound negative ions (such as Ca^-) are rather easily made by (sequential) double electron capture of positive ions in, e.g., alkali vapor [PAB96]. Negative ions to be studied in ion traps are normally produced by dissociative electron attachment to a suitable gas. Mass analysis is an indispensable part of negative ion spectroscopy. Precise knowledge of the ion energy is normally not required when keV ion beams are used from sources with energy spreads in the 1–10 eV range. In the following discussion, we concentrate on photodetachment spectroscopy with collimated negative ion beams (energies typically in the range 100 eV–100 keV).

(ii) Since negative ion ensembles can only be formed as low density targets, use of lasers or laser-based coherent radiation with their high photon flux (at narrow bandwidth) is mandatory for high resolution studies of negative ions. In most cases pulsed tunable dye lasers (including frequency doubling) with bandwidths between 0.05 and 1 cm^{-1} have been used for threshold photodetachment studies in the rang 300–950 nm. Quite recently, intense coherent infrared radia tion, produced by first or second order Stokes Raman shift ing of tunable dye lasers in a molecular hydrogen cell ha been applied to investigate thresholds in the region beyon 950 nm (photon energies 2000–10000 cm^{-1}) at bandwidth around 0.1 cm^{-1} (see Sec. 4.1). Use of pulsed lasers in con junction with time-gated product detection results in hig signal-to-noise ratios because the cw background due to de tachment in collisions with residual gas is strongly discrimi nated. Care has to be taken, of course, that saturation of th photodetachment process (which occurs at photon fluence Φ_γ above about $0.1/\sigma$, σ = photodetachment cross section) i avoided.

cw single mode lasers offer the highest resolution, bu their use requires efficient measures to reduce collisional de tachment by applying ultrahigh vacuum environments. Wit the advent of titanium–sapphire lasers (700–1000 nm) a intense broadly tunable cw light source in the infrared be came available, which is superior to cw dye lasers in thi range. Yet, cw lasers are generally harder to work with ove extended wavelength ranges (especially under single mod operation) than are pulsed lasers. Moreover, there are limita tions for cw dye lasers towards shorter wavelengths, includ ing low efficiencies for frequency doubling.

(iii) Efficient detection of the products from reaction (3.1 is a key component of a successful photodetachment experi ment. In the case where one is simply interested in the tota detachment yield, detection of the atoms by electron emis sion from a surface in combination with an electron multi plier is an efficient means of monitoring the process whe negative ions of sufficient kinetic energy are used. An alter native may be sampling of the photodetached electrons, bu this requires application of an electric field in the photode tachment region which may influence the photodetachmen process [GR88]. In threshold studies it may be advantageou to sample very slow electrons with high efficiency, whil faster electrons from open channels are strongly discrimi nated against. Several variants (extraction by weak, penetrat ing electric fields [SRN78, FBH78]; low energy electro guide with weak magnetic field [MLL84]) have been used. A powerful new development involves state-specific neutra atom detection by resonance ionization (see Sec. 4.2).

In LPES high resolution electron energy analyzers are re quired to determine binding energies with uncertainties be low 10 meV [HL85]. So far electrostatic analyzers, detectin electrons in a direction essentially perpendicular to the lase and ion beam directions, have been mainly used in studies o atomic negative ions in conjunction with intense cw laser (514.5 or 488.0 nm multimode argon ion laser with intracav ity operation; single mode 351 nm argon ion laser in con junction with buildup cavity [EHL88]). With pulsed lasers, natural alternative is offered by time-of-flight (TOF) energ analyzers, including the option of 2π detection with a mag netic bottle spectrometer [KR83]. This option may prove es pecially useful in investigations of atomic negative ions wit low binding energies when pulsed, Raman-shifted, infrare

radiation is used to create electron spectra at low energies where TOF analyzers offer the highest resolution.

3.3. Laser Photodetachment Threshold Studies (LPT)

The determination of (EAs) is accomplished by measuring the threshold photon frequency of the transition from the negative ion ground state to the ground state of the neutral atom plus a threshold electron (zero energy in the center-of-mass frame of the negative ion). Sometimes it is favorable to measure the onset due to the formation of an excited state A^* of the neutral and subtract the (normally accurately known) excited state energy of A^*. Assuming that the observed transition is identified without ambiguity, the determination of the threshold position from the frequency dependence of the detachment product rate involves only an extrapolation based on a known threshold law. According to Wigner [Wi48], the leading term in the energy dependence of the photodetachment cross section $\sigma(\nu)$ is given by

$$\sigma_L(\nu)=a_1(\nu-\nu_{\mathrm{THR}})^{L+1/2}=a_2\varepsilon^{L+1/2}=a_3k^{2L+1}. \qquad (3.4)$$

Here ν is laser frequency, ε, k is the energy and wave vector of the photoelectron (in center-ofmass), L is the orbital angular momentum of the photoelectron, and a_1, a_2, a_3, are constants. Resonances near threshold are assumed to be absent. The energy range over which Eq. (3.4) provides a valid description of the threshold behavior is not known from theory, but estimates are possible through the consideration of correction terms, associated with the long-range interactions between the electron and the atom A. Neglecting permanent multipole moments of the atom, the leading interaction is the polarization attraction $V_{\mathrm{pol}}(r)=-\alpha/(2r^4)$ (in atomic units; α= static polarizability of atom A); it produces a multiplying correction term $p(k)$ to the basic threshold law, Eq. (3.4), which reads as follows [Ma65, HPL73]:

$$p(k)=1-4\alpha k^2\ln k/[(2L+3)(2L+1)(2L-1)] +O(k^2). \qquad (3.5)$$

Here all quantities are to be taken in atomic units and $k \ll 1$. Note that the sign of the α-containing term was incorrectly given in [Ma65], as noted under Ref. 20 in [HPL73]. Although the last term in Eq. (3.5) is of the same order as the second term, evaluation of the second term alone has proved useful (see, e.g., [HPL73, HL73]) to estimate how close to threshold significant deviations (of order 10%) from the basic threshold law, Eq. (3.4), may be observed. Note that the second term is negative for $L=0$ (s-wave detachment), but positive for $L\geq 1$ as discussed in [HPL73, HL73]. It is expected from Eq. (3.5) that for final atomic states with high polarizabilities (e.g., for Rydberg states) the Wigner law, Eq. (3.4), will be valid only over a narrow, sub-meV wide energy range in agreement with experimental observations [SRN78, FBH78]. Using the zero-core-contribution (ZCC) model of photodetachment [SW79], Farley [Fa89] has estimated the size of correction terms to the Wigner law, Eq. (3.4), which in some cases allowed a description of the photodetachment threshold behavior over wider energy ranges (e.g., for B^- detachment [SBH98b]), but this procedure does not appear to work in general. To be sure of the validity of the extrapolation to threshold, data should always be taken at sufficiently high resolution with a narrow-frequency grid over a region where the basic law, Eq. (3.4), provides a good description.

From Eq. (3.4) it is obviously desirable to look at an s-wave threshold ($L=0$) (infinite derivative at threshold) in order to achieve optimal conditions for an accurate determination of the transition energy. Within the electric dipole approximation, s-wave detachment requires that the parities of the initial negative ion state and the final atomic state are different and that the respective total angular momentum quantum numbers differ by no more than 3/2. As an example, we note that the lowest energy s-wave threshold for photodetachment of negative alkali ions Ak^- ($ns^2\ ^1S_0^e$) requires formation of excited $Ak^*(np_J)$ atoms, and these thresholds have in fact been exploited for the most precise determinations of the EAs for the alkali atoms [SRN78, FBH78, HHK96]. It should be noted, however, that even p-wave ($L=1$) thresholds have allowed measurements of EAs with uncertainties $\approx 0.2\,\mathrm{cm}^{-1}$ [LML91, BSH98], at least in favorable cases. The error bars reflect the total uncertainties calculated from the known individual contributions. Particularly for p-wave thresholds, which are very sensitive to baselines and slope changes near threshold, the EA values may prove optimistic if unknown systematic effects are sufficiently significant to have influenced the measurements.

Apart from the necessary extrapolation to threshold, another critical aspect of any accurate determination of the binding energy is the precise measurement of the photon frequency. Before we dwell on this point further, we note that the frequency ν_{Lab} in the laboratory frame is connected with the frequency ν, as witnessed by a moving ion (velocity v relative to laboratory) in its rest frame, by

$$\nu=\nu_{\mathrm{Lab}}(1-(v/c)\cos\alpha)/[1-(v/c)^2]^{1/2}. \qquad (3.6)$$

Here, the angle α encloses the propagation directions of the ion and laser beams ($\alpha=0$ for parallel ion and photon beams). Depending on the experimental geometry and ion velocity, the lab threshold frequency will differ more or less from the EA frequency $\nu_{\mathrm{EA}}=\mathrm{EA}/h$, needed to promote electron detachment in the ion rest frame. For setups with collinear ion and laser beams it is mandatory to determine threshold frequencies $\nu_{\mathrm{Lab},p}$ for parallel and $\nu_{\mathrm{Lab},a}$ for antiparallel ion and laser beams in order to take advantage of the fact that ν_{EA} is then simply obtained from [JBB85, KPR85]

$$\nu_{\mathrm{EA}}=(\nu_{\mathrm{Lab},p}\cdot\nu_{\mathrm{Lab},a})^{1/2} \qquad (3.7)$$

in a way independent of the ion velocity (as long as the ion velocity is the same for the two measurements with parallel and antiparallel beams). This approach is preferable to the use of the formula [HL85]

$$\nu_{\mathrm{EA}}=(1/2)(\nu_{\mathrm{Lab},p}+\nu_{\mathrm{Lab},a})[1-(v/c)^2]^{1/2}, \qquad (3.8)$$

even though the uncertainty in the second-order correction term in Eq. (3.8) is normally so small that Eq. (3.8) yields results with the same precision as those obtained from the geometric means in Eq. (3.7). In this connection we mention that the minute threshold shift associated with the recoil, transferred to the electron–atom system by the absorbed photon, is several orders of magnitude smaller than the uncertainty of the best experimental threshold determinations. The effect is largest for $^1H^-$ and $^{19}F^-$ photodetachment (about $3\cdot10^{-10}$ eV).

In experiments carried out with perpendicular ion and laser beams care has to be taken to avoid the first-order Doppler effect (by choosing $\alpha=90°$) or to ensure precise knowledge of the angle α otherwise. An elegant approach to eliminate the influence of the first order Doppler effect for (nearly) perpendicular laser and ion beams has been demonstrated by Blondel *et al.* [BCD89] in precision measurements of the EAs of F^- and Br^- ions. Using a corner cube reflector they generated two interactions of the pulsed laser beam, spatially separated by 1.4 cm, with the negative ion beam in such a way that the incident (i) and returning (r) laser wave vectors were exactly antiparallel. Therefore, the first order Doppler shifts in the two interactions had the same absolute value, but opposite signs. The detachment signals from the two interactions were separated by TOF, allowing the thresholds from the two interaction regions to be individually sampled. The EA transition frequency in the ion's rest frame was obtained from

$$\nu_{EA}=(1/2)(\nu_i+\nu_r)[1-(v/c)^2]^{-1/2}, \qquad (3.9)$$

with relative uncertainties of 0.9 ppm (F) and 0.6 ppm (Br) [BCD89].

Precision measurements of the laser (vacuum) wavelengths are mandatory for accurate EA determinations. For cw single mode lasers traveling-wave Michelson interferometers involving polarization-stabilized HeNe lasers and integer fringe counting can be routinely used at relative uncertainties down to about 3×10^{-7}, once the HeNe laser has been accurately calibrated. With fringe interpolation techniques the performance can be improved by more than a factor of 10, but great care has to be taken to ensure optimal optical alignment. For nonevacuated wave meters, corrections for the influence of the wavelength-dependent index of refraction of the gaseous medium (typically air) [Bö98] are mandatory. Multimode cw lasers or pulsed lasers are normally characterized by a wavelength comparison with a calibration system, e.g., by absorption in molecular iodine vapor ([VDH98] and references therein) or by optogalvanic spectroscopy of atomic transitions [BBS90]) in conjunction with wavelength markers from a calibrated Fabry–Pérot interferometer or étalon. It is difficult to achieve uncertainties much below the laser linewidth which for good pulsed lasers is typically ≥0.05 cm^{-1}. So far Fourier-transform limited, pulsed lasers (bandwidth down to 0.002 cm^{-1} for ns laser pulses) which involve injection seeding of pulsed amplifiers with cw single mode lasers have been rarely used in photodetachment threshold experiments for measurements involving a pulsed laser with a width of a few 0.001 cm^{-1} (se [BCD89]).

3.4. Laser Photodetachment Electron Spectrometry (LPES)

In the preceding review [HL85] most of the reporte atomic EAs were based on LPES, and therefore this subje was discussed in some depth. The reader is referred to Sec. in [HL85] for details. Since that time this method has bee exploited by several groups for measurements of binding e ergies in negative ions of molecules as well as molecular an metallic clusters [CB96], but it has added rather little to th knowledge of atomic negative ions. As a remarkable exce tion we note the discovery of stable Ca^- ions [PTC87] whic involved energy analysis of photodetached electrons, emitte parallel and antiparallel to the direction of a 70 keV Ca beam. Although care was taken to account for the relevai kinematic effects associated with the transformation from th ion's rest to the laboratory frame (see discussion in [HL85 the quoted value for the EA of Ca (43(7) meV) [PTC87 which agreed well with the theoretical prediction of 45 me reported in parallel work [FLV87], was later proven to be to high by about 20 meV by s-wave photodetachment threshol spectroscopy [PAB96]. A similar discrepancy was observe for Be^- [TWP93, KPA 95] as discussed in connection wit Table 1 (see Sec. 2).

LPES is a powerful exploratory method and best suited t provide solid initial information on the level structure an binding energies in negative ions at uncertainties around 1 meV or even below, as demonstrated by measurements o the negative ions of Ge and Sn [MSL86] as well as Fe an Co, [LL86] which yielded electron affinities with 3–4 me error bars. LPES also provided improved values for the ele tron affinities of Ga [WCC98a], In [WCC98b] and A [LXL98]. It was hoped in 1985 [HL85] that LPES woul soon shed light on the EAs of lanthanides and actinides, b apart from recent work on La^- [CCT98], these negative ior have not been investigated by LPES (or by LPT spectro copy) up to now.

4. New Developments in Negative Ion Spectroscopy

4.1. Tunable IR Laser Photodetachment Spectroscopy

Nonlinear optical techniques have been employed exte sively in recent years, for accessing new wavelength regim as well as for the application of multiphoton absorption pr cesses in spectroscopic investigations. In light of the lo binding energies of negative ions, tunable infrared light very useful in photodetachment studies to the ground state the neutral atom, while tunable ultraviolet light is often r quired in resonant ionization spectroscopy (Sec. 4.2) as we as in threshold measurements on the few strongly bou atomic negative ions [BCD89, BGH95, HG92]. Tunable i

frared laser spectroscopic techniques have been applied to single photon threshold detachment of a number of atomic negative ion species in the past few years in a crossed laser-ion beam geometry [BSH98, NBB99, SBB98a, SBB98b, SBH98b, SBT98, SHB97, TSS96b]. These works employed a pulsed dye laser pumped by a Nd:YAG laser. The system operates at a repetition frequency of 10 Hz, and has a nominal pulse energy of the Nd:YAG 532 nm pump light of 400 mJ in a 8 ns pulse. The dye laser itself yields wavelengths up to 980 nm, with typical laser pulse energies of 50 mJ at 700 nm and 25 mJ at 980 nm. The linewidth of the dye laser varies from 0.1 to 0.06 cm^{-1} over this range. Given a Raman shift in a high-pressure hydrogen cell (at 22 bar) of 4155.187(5) cm^{-1} [BD86], the first Stokes light falls in the wavelength range of 950–1650 nm. The second Stokes light is in the range of 1.6–5.2 μm, but in a simple high pressure cell, this output often suffers from the lower (spatial) beam quality associated with four-wave mixing [SBB98a, BSH98]. Output pulse energies of the Raman-converted laser beams range from several milliJoules at a wavelength around 1 μm to values around 100 μJ at a wavelength of 5 μm. Strong atmospheric absorption in some infrared spectral regions has necessitated purging of the entire beam path subsequent to the nonlinear optical conversion step in the high pressure hydrogen cell [STB98]. A sputter ion source, yielding ion beam currents often in the tens or hundreds of nanoamperes in the ultrahigh vacuum (10^{-9}–10^{-8} mbar) laser ion–beam interaction region, provides intense and highly stable beams of many atomic species. Despite the very small effective duty cycle of laser–ion beam interaction (determined either by the laser pulse length or by the ion transit time through the transverse dimension of the collimated laser beam), and the small photon–ion cross sections, the signal-to-noise of the photodetachment threshold measurements is often excellent. This aspect is explained by the fact that the laser pulse energies and ion beam currents usually translate into at least one detected neutral particle per laser pulse. Discrete dynode electron multipliers, which can exhibit excellent linearity over a wide dynamic range, can be utilized to accept signals corresponding to several detached particles per laser pulse, thereby effectively utilizing the available signal at the low pulse repetition rate of 10 Hz. This signal level, combined with the very low backgrounds associated with the ultrahigh vacuum conditions, means that time-gated measurements at 10 Hz have proven to be a most viable measurement approach.

These parameters have proven to be entirely adequate for the studies reported in the past couple of years (an example is presented in Fig. 1), but for future work, great improvements in the laser capabilities can be expected (see Sec. 9). The accuracy of the tunable infrared laser photodetachment studies is limited by a variety of factors including the residual Doppler effects, calibration uncertainties, laser tuning nonlinearities and temperature sensitivities, and the laser linewidth. Improvements in these pulsed laser techniques may push the accuracy limits on ionic binding energies even further, although achieving an additional order of magnitude

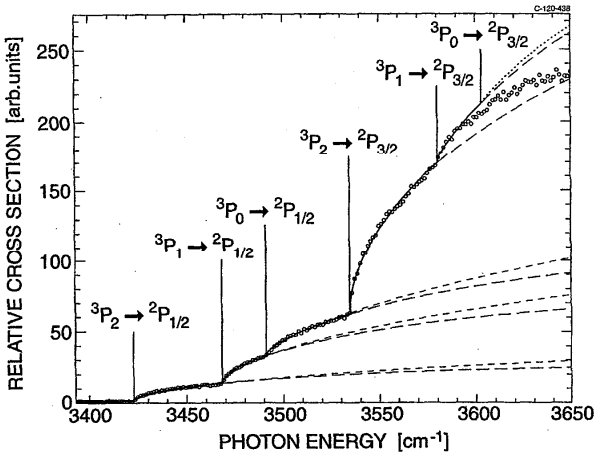

FIG. 1. Photodetachment yield vs photon energy for the Al^- ion [SBT98]. The measurements are performed by tunable infrared spectroscopy. The data are analyzed using a Wigner s-wave fit including the leading correction term (solid line). For the first three thresholds the difference between the dotted lines represents the contribution from the correction term. Thus, the two lines define the upper and lower limits for the s-wave thresholds.

is a challenging goal for experimentalists. (High resolution pulsed laser techniques in a collinear regime, and using visible light, have achieved an accuracy of about 0.05 cm^{-1} [HKR96].) For single photon studies, future advances in tunable IR laser technology could be usefully applied to, for example, the negative ions of Sc, Fe, Ga, As, a number of transition metals of intermediate mass, In, the rare earths, Ta, Re, Tl and Pb.

4.2. Laser Photodetachment Threshold Studies Involving Resonance Ionization Detection

For the determination of EAs of negative ions with binding energies below about 150 meV the general lack of tunable lasers in the mid-to-far infrared region (Sec. 4.1) makes it necessary to rely on alternative methods. The binding energy determination can be performed by measuring the photon energy between the negative-ion state and an excited state in the neutral atom, for which the excitation energy is known. This method has been used for many years, but the accuracy of the determined electron affinities was considerably lower [HL85] than could be obtained with detachment to the ground state. The reason was that changes in the photodetachment cross section, from the opening of a new detachment channel, would be superimposed on the large photodetachment cross sections for the lower-lying atomic states. Since the opening of a new detachment channel with $L \geqslant 1$ can be difficult to identify with good accuracy, relying on conventional detection of the total number of neutral particles formed by photodetachment [HL85], a significant improvement could be obtained by utilizing $L=0$ channels (Sec. 3.3) and by combining this approach with the very sensitive resonant laser photoionization method [AKL91] to probe the opening of a new detachment channel.

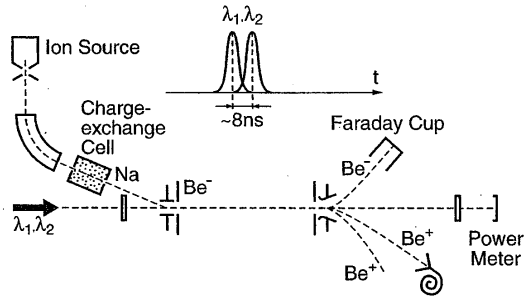

FIG. 2. Schematic diagram of the experimental setup for laser photodetachment threshold spectroscopy of the Be^- ion utilizing resonant ionization detection ([KPA95, AAB97]).

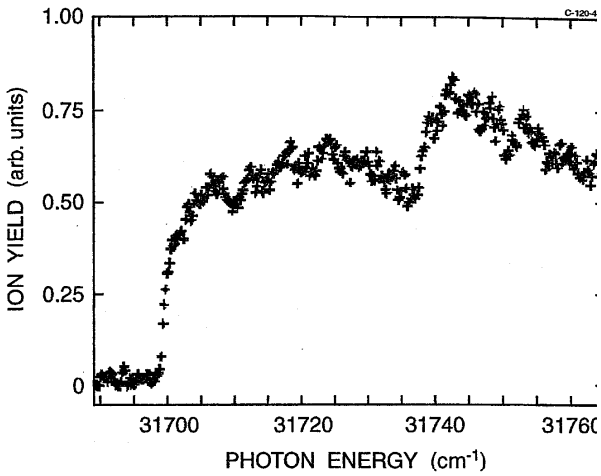

FIG. 3. Determination of the binding energy and fine structure splitting $Ca^-(4s^24p\ ^2P_{1/2,3/2})$ ions by laser photodetachment spectroscopy at t $Ca(4s5s\ ^3S_1)$ threshold in combination with resonant ionization detectic [PAB96].

This method, which originally was developed for rare isotope detection, facilitates the distinction between close lying photodetachment channels as well as between different negative-ion states. Detection of an excited neutral atom state using resonant ionization spectroscopy (RIS) offers the following advantages: high efficiency, very high optical selectivity, and strong suppression of the collisionally induced background (below 10^{-7} at 10^{-7} mbar). This technique has been applied to determine the electron affinities for a number of ions such as He^- [KPP97], Li^- [HHK96], Be^- [KPA95, ABP96], K^- [ASK99], Ca^- [PAB96], Sr^- [APK97], and Ba^- [PVB95].

Figure 2 shows a schematic drawing of the experimental setup for measuring binding energies of the weakly bound alkaline–earth ions. The negative ions are formed by charge exchange of fast positive ions, and after elimination of the neutral and remaining positive components, the negative beam is overlapped collinearly with two pulsed laser beams (λ_1 and λ_2) in a 1 m long field free interaction region. The first laser field is applied to detach the negative ions, applying photon energies in the threshold region for production of neutral atoms in an excited neutral-atom state. The second laser field is used for excitation of the specifically produced neutral atom state to a Rydberg state, which subsequently is selectively field ionized and detected as a positive ion.

The demand that the emitted electron should have zero angular momentum often results in the use of rather weak detachment channels. Using Ca^- as an example, the $4s^24p\ ^2P$ ground state was photodetached to the $4s5s\ ^3S_1$ state in neutral Ca [PAB96], a process which requires interelectron correlation. The opening of the detachment channel was monitored by laser excitation of the $4s5s\ ^3S_1$ state to the $4s15p\ ^3P_2$ Rydberg state followed by state-selective field ionization of the $^3P_2$ state. The signal detected for the $Ca(4s5s\ ^3S_1)$ level corresponds to approximately 0.1% of the detached Ca^- ions. Figure 3 shows the recorded Ca^+ production following the photodetachment of the Ca^- ground state. Figure 3 illustrates the accuracy (0.10 meV) by which the binding energies of the two ^2P fine structure components could be determined, an improvement by a factor of 25 compared to previous laser photodetachment studies [WP92]. In addition, the fine structure splitting, which can easily be seen in the figure, was observed for the first time.

For the He^- ion [KPP97], it has been possible to improve th accuracy still more using this technique (0.006 meV).

The presence of two metastable states in the negative be ryllium ion, $2s2p^2\ ^4P$ and $2p^3\ ^4S$, which are connected b an optical transition, has made it possible [ABP96] to furth develop this technique. The state-selective, stepwise tw photon detachment method, combined with resonant ioniz tion detection, has allowed information to be obtained abo the fine structure splittings of the ^4P_J levels and the lifetim of the $J=1/2$ and 5/2 levels. The lifetimes have values in th range 0.1–1 μs, a lifetime region which previously was i accessible for negative ion studies (see also Sec. 4.5).

The state-selective detection method also plays an impo tant role in nonlinear laser techniques developed to gain i formation about excited states in negative ions [KBP9 PBK98]. In addition, state-selective depletion spectroscop [KBP97] has yielded fine structure splittings with high acc racy for ions as Ca^- and Sr^-.

4.3. Resonant Multiphoton Detachment of Negative Ions

Until very recently, multiphoton techniques had not bee routinely applied to negative ions. After an early (nonres nant) two-photon detachment experiment [HRB65] the inte est of experimentalists was again stimulated in the late 198 and early 1990s, aimed at first toward strong laser field stu ies in these qualitatively different systems [DMH91, BCD9 SBB91]. More recently, resonantly enhanced multiphoton i teractions have been demonstrated. Beyond the stimulate Raman scheme discussed in more detail below (Sec. 4.4 two different approaches have been utilized: a 1+1 photo detachment process via a magnetic dipole ($M1$) bound bound transition in the first step [TSS96c, SHB97, SBH98 SBB98b], and a 2+1 photon detachment scheme [SHB97 where the first step involves the absorption of two photons i

an electric dipole (E1) allowed two-photon transition, followed by single photon detachment of the upper level. The 1+1 $M1$ process is well suited for negative ion studies since all of the bound levels experimentally identified to date in negative ions are levels of the same parity. The 1+1 photon absorption scheme allows an intense laser pulse to transfer significant population between two levels of the same parity, and the subsequent detachment step facilitates very efficient detection. Nonlinear optical conversion techniques, often via stimulated Raman conversion in a high pressure hydrogen cell, provide access to a range of infrared wavelengths suitable for studies on weakly bound negative ions. The typical laser and ion beam characteristics associated with these infrared multiphoton experiments have been outlined in Sec. 4.1.

The initial demonstration of this approach led to the first experimental determinations of selected fine structure splittings in Ir^- and Pt^- [TSS96c]. The accuracy is limited by factors including the laser linewidth, the residual Doppler effect in the transverse ion beam/laser beam geometry, and the calibration of the laser wavelength. The measurement leads to a sharp resonant peak and thus highly accurate energy level determinations with relatively little chance of systematic errors. This stands in contrast to Wigner thresholds, particularly those other than s-wave character, where the extrapolation to threshold can be influenced by background levels on the baselines. Accuracies on the order of 0.2 cm^{-1} are obtained with the multiphoton approach. Another important advantage of the resonant multiphoton techniques is that population is transferred into and out of excited levels that may not otherwise be significantly populated from the ion source. Thus a one-photon threshold detachment experiment from an excited level may prove impossible if the level has virtually no thermal population, whereas strong signals can often be obtained in the multiphoton regime. Laser intensity effects must be taken into consideration, but it can be shown that these issues are negligible for the multiphoton based studies conducted to date [Sc98].

Following the initial work on Ir^- and Pt^-, a number of other multiphoton experiments have been conducted. The application of $M1$ resonances was confirmed in a very convincing way in the case of Te^-, where the fine structure splitting was already known with high accuracy, and the A coefficient was also relatively well known [SBH98a]. This work on the negative ion of tellurium led to the realization of the existence of a minor calibration error in previous stimulated Raman based studies on this system. A "complete" study on the negative ion of antimony [SHB97], using both single and multiphoton (1+1 and 2+1 photon absorption) approaches, led to much improved data on this ion. Figure 4 shows schematically the various excitation methods used in the study of the Sb^- ion.

$M1$ resonances have also been observed for the $^4S_{3/2}-^2D_J$ transitions in Sn^- [SBB98b]. Several (unsuccessful) careful searches, using both 1+1 and 2+1 photon absorption schemes in Si^-, have been applied in attempts to observe the ^2P_J levels of this ion [SBB98b]. Both the ^4S and ^2D_J states

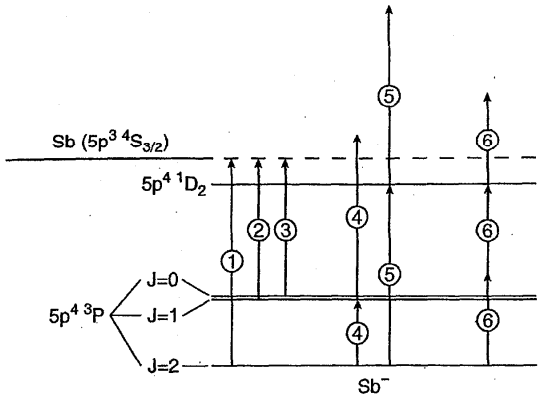

FIG. 4. Schematic energy level diagram of Sb^-. Arrows indicate different photodetachment schemes: (1–3) single photon detachment thresholds; (4–5) two-photon detachment via single-photon $M1$ resonance; (6) three-photon detachment via two-photon El resonance [SHB97].

were used as initial levels in these searches. The ^2P_J levels of Si^- are currently known only to an accuracy of 5 meV and a resonant multiphoton experiment would lead to a large improvement. Also, attempts to drive the $^4S_{3/2}-^2D_{3/2}$ $M1$ transition in Ge^- remain unsuccessful [SBB98b]. The weak transition strengths, in part due to the quartet-to-doublet spin changes, are deemed responsible for the lack of observed signals in these cases. The 2+1 photon absorption scheme has so far only been successfully applied to the $^3P_2-^1D_2$ transition in Sb^-. There are a large number of possible future experiments based on multiphoton techniques which could greatly enhance our knowledge of atomic negative ions.

4.4. Stimulated Raman Scattering Detachment Spectroscopy

The first resonant multiphoton technique to be applied to a negative ion was a 2+1 photon absorption experiment to determine the $^2P_{3/2}-^2P_{1/2}$ splitting in Te^- [KSB93]. In this case, two laser fields are utilized in a scheme whereby the energy difference of the photons is close to the fine structure separation to be measured. One of the laser fields is fixed in wavelength, while the other is tuned over an appropriate range. The more energetic photons will be referred to as "blue" and the less energetic as "red." The first step in the photodetachment process is a nonresonant two-photon ($E1$ allowed) transition between the two levels involving both a red and a blue photon. The second step is a single photon detachment process from the upper fine structure level, resulting from the absorption of one photon from the blue laser beam. To date the 2+1 stimulated Raman scattering technique has only been successfully applied to the negative ions of selenium and tellurium [TSS96a], see Fig. 5. As with other multiphoton experiments (see Sec. 4.3), the Raman technique leads to a sharp resonant peak in the experimental signal, and facilitates highly accurate measurements down to a level of ~0.2 cm^{-1}. The Raman approach also transfers population between levels and thus can lead to measurements on states which would not be significantly populated

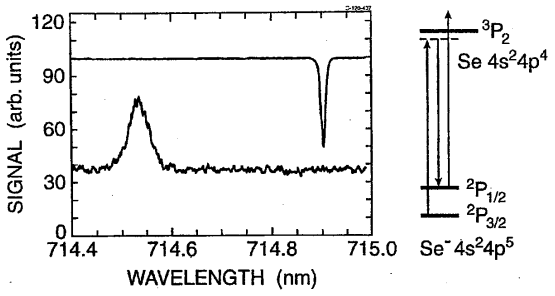

FIG. 5. Raman photodetachment of $Se^-(^2P_{3/2})$ ions [TSS96a]. An illustration of the (2+1) Raman-detachment scheme is shown on the right side. The neutral Se atom signal vs the wavelength of the "red" laser is shown in the lower trace, while the wavelength of the "blue" laser is fixed at 614.476 nm. The optogalvanic calibration signal is shown in the upper trace.

in the ion source. However, this aspect is not generally as important in the Raman case as in the other multiphoton schemes since the Raman approach is most naturally suited to measurements on levels that are not very highly excited. The background in these experiments is due to single photon detachment by the blue laser beam of any thermal population in the upper level, nonresonant two-photon detachment by either beam, as well as collisional detachment. The present approach can be seen as being very complementary to the other multiphoton techniques.

The stimulated Raman process was the basis for the best measurement of the $^2P_{3/2}-^2P_{1/2}$ splitting in Te^- [KSB93]. The Raman-based experiment in Te^- was later shown to suffer from a minor dye laser calibration error; hence the 1 +1 $M1$ multiphoton experiment currently defines the fine structure splitting in that ion [SBH98a]. The 2+1 photon Raman experiments were also attempted in Ir^- and Pt^-, in order to help verify the interpretation of the proposed 1+1 $M1$ resonances observed in those systems [TSS96c]. However, the Raman experiments were unsuccessful in the iridium and platinum negative ions. The reasons for this are not yet clear, but could be due to a much smaller multiphoton cross section in these cases.

Future experimental work on the atomic negative ions should attempt the 2+1 photon Raman scheme in a wider range of species. Some of the transition metal elements would provide excellent test cases. It would also be interesting to explore the possibility of conducting such experiments in cases where one or both laser beams have photon energies exceeding the detachment threshold. In these cases, laser pulses in the 5–10 ns duration range would not generally be viable, but rather, short-picosecond light pulses would be much more suitable. In this way, the transition probability might be greatly enhanced, allowing measurements to be done without an excessive one-photon absorption background, while still maintaining acceptable laser linewidth near the Fourier transform limit. The stimulated Raman approach has also been successfully applied to studies of C_2^- [BZY95], indicating that there may be many applications for molecular species.

4.5. Metastable Negative Ions Studied by Storage Rings

Negative ions, which can retain their extra electron for a indefinite period of time, are considered stable. Additiona energy is required to remove the extra electron. Stable ion with binding energies below 150–200 meV will, however be destroyed in less than 100 ms at room temperature due t the interaction with blackbody radiation. Ions which are nc stable but hold on to their extra electron for more tha $10^{-6}-10^{-7}$ s, making them suitable for beam experiments are considered metastable. Negative ions with shorter life times may manifest themselves as resonances that usuall decay via electron emission, but optical emission can, if elec tron emission is prohibited, be the preferred decay mode, a observed for the Li^- [MAK80] and the Be^- [GA89] ion.

Before the 1985 review [HL85], detailed lifetime studie of metastable negative atomic ions had only been performe for the He^- $(1s2s2p\ ^4P)$ ion. This ion exhibits differentia metastability with respect to autodetachment. The $J=1/2$ an 3/2 levels decay by spin–orbit and spin–spin interactions whereas the $J=5/2$ state decays only by spin–spin interac tion. Utilizing a 10 m long beam line, Blau *et al.* [BNW7C determined the various J level lifetimes using a TOF tech nique, measuring the negative ion intensity at different posi tions along the beam direction. For lifetimes much longe than 10 μs the single-pass setup only allows a very limite part of the metastable beam to decay. In 1990 heavy-io storage rings, dedicated to atomic and molecular physics became available and eliminated this problem. It was the possible to observe a circulating negative beam for period of seconds, making TOF studies feasible for metastabl negative ions with lifetimes in the range from 10 μs to 10 ms [BAA92, AAB93, AAH97]. The short time limit was se by the round-trip time of the ions in the ring and the lon time by the negative ion-rest gas collisions (at a pressure a low as 3×10^{-11} mbar) leading to destruction of the ion.

The decay of the negative ions circulating in the storag ring can be measured with a detector which monitors th fast, neutral atoms produced along one straight section of th ring. The advantages of using a storage ring rather than single-pass beam to study lifetimes of metastable negativ ions are: data can be extracted over a much greater tim range, out to several lifetimes, with a good signal-to-nois ratio; slit scattering is essentially eliminated in the ring; an the ultrahigh vacuum conditions render collisional quenchin entirely negligible. The possible mixing of magnetic substat populations, caused by the steering quadrupole magnets, ma be considered as a disadvantage for the storage ring tech nique [AAH97]. Lifetime measurements of metastable nega tive ions have also been performed using an electrostatic io trap, which stores keV ion beams using electrostatic field only [WBB99]. This technique can eliminate the complica tion of the magnetic-induced mixing effects observed at sto age rings [AAB93].

Storage rings have also proved valuable to gain prelimi nary information about the binding energy of weakly boun

negative ions, which are sensitive to photodetachment by blackbody radiation [HAA92, PVB95, STB98, AAP98]. The Ca^- ion, with a binding energy of only 24 meV [PAB96], exhibits a lifetime for survival at room temperature of 500 μs [HAA92].

4.6. Other Methods: Laser Photodetachment Microscopy (LPM); Accelerator Mass Spectrometry (AMS)

LPM is dealing with photodetachment of atomic anions in the presence of a uniform electric field [BDD96, BDD99]. Information can be obtained about the spatial distribution of the emitted electrons around the electric field axis. It has been possible to directly visualize the nodes and antinodes of the parabolic wave function of the emitted electron and thereby to gain some knowledge about its radial nature. The possible use of photodetachment microscopy for accurate determinations of electron affinities has been investigated [VBD99] utilizing the ^{16}O and ^{18}O isotopes as test cases. The results will be discussed in Sec. 5.6.

Accelerator mass spectrometry (AMS) using tandem accelerators has proved to be a valuable tool for studies of negative ions, particularly for elements for which the experimental evidence has not yet been established. Examples are the lanthanides and the actinides [NGZ97]. AMS can yield unambiguous identification of the atomic ion and of its mass. Information about the EA for a given element can, for a weakly bound negative ion as Ca^- [NZG92], be obtained from investigation of the survival property of the negative ion towards the electric-field dissociation taking place during acceleration and focusing. This technique has produced the first EA values for elements like Tm and Dy [NGZ97].

5. Survey of Electron Affinity Determinations Including Theoretical Results

In this section we provide brief discussions on the present status of EA determinations, ordered by atomic subgroups, and emphasize progress made since 1985.

5.1. Hydrogen and Alkali Atoms (H–Cs) (Z=1, 3, 11, 19, 37, 55)

The best known EA of all elements is that of hydrogen, as obtained by elaborate numerical calculations mentioned in Sec. 2. Relative to the H ($1s$, $F=0$) hyperfine level, the H^- ion is predicted to be bound by 6083.064 145(30) cm^{-1} [Dr99]. Since 1985 two LPT experiments have tried to establish an accurate experimental number for EA[H($1s$)]. Lykke *et al.* [LML91] used a cw color center laser (0.5 W, bandwidth 1 GHz) to study threshold photodetachment from a 2.7 keV H^- beam, collinear with the laser beam. From the two threshold frequencies, determined for parallel and antiparallel beams, they deduced the value EA[H($1s$, $F=0$)] $=6082.99(15)$ cm^{-1}. They also studied D^- ions with the result EA[D($1s$, $F=1/2$)]$=6086.2(6)$ cm^{-1}. Within the error margins, these results agree with the more precise theoretical values. We note that from the thresholds for H^- photodetachment, marked in Fig. 3 of [LML91], one obtains an electron affinity which is 0.2 cm^{-1} lower than the numerical result given in [LML91]; this indicates that the photon frequency scale in Fig. 3 needs recalibration by this amount.

In a more recent experiment involving H^- ions stored in a Penning trap, Harms *et al.* [HZG97] investigated threshold photodetachment with a single mode color center laser (50 mW) and obtained EA(H)$=6082.8(7)$ cm^{-1} in agreement with theory and Lykke *et al.* [LML91]. Several improvements of this experiment are possible to obtain a better statistical quality, to reduce the influence of the Doppler broadening, and to characterize in detail the effects of the magnetic and (motional) electric field. It appears difficult, if not impossible, however, to reach a level of precision sufficient to compete with that of the theoretical calculation.

The most accurate determinations of the EAs of the alkali atoms Ak involve studies of threshold photodetachment to an excited atomic state accompanied by emission of an s-wave photoelectron, e.g.,

$$Ak^-(ns^2S^o_0)+\gamma \rightarrow Ak^*(np^2P^o_J)+e^-(\varepsilon s). \quad (5.1)$$

Selective detection of this channel is achieved by monitoring the threshold electrons [SRN78, FBH78] or state-selective detection of the excited atom A*, preferably by the highly sensitive method of resonance ionization (see Sec. 4.2). The latter technique was recently applied to Li^-, using two pulsed tunable lasers interacting with a collinear ion beam [HHK96]. The overall resolution amounted to almost 0.2 cm^{-1}; from the geometric mean, Eq. (3.7), of the two threshold laboratory frequencies, measured for parallel and antiparallel ion and laser beams, and subtracting the known excited state energy (here of Li($2p\,^2P^o_J$)), the authors obtained EA(Li)$=4984.90(17)$ cm^{-1}, a value 24 times more accurate than the 1984 value [HL85]. The same method was very recently applied to K^-, yielding EA(K) $=4044.54(10)$ cm^{-1} [ASK99] and thereby reducing the uncertainty of the previous (identical) value [SRN78] by a factor of 8.

For Na^-, Rb^-, and Cs^-, the values given in [HL85] are still relevant. The numbers listed in Table 3 were recalculated from the 1985 values using the proper eV cm^{-1} conversion factor [Ta 99]. For Cs^-, a recent high resolution study of the Cs^- ($6s^2\,^1S^e_0$)$\rightarrow$Cs($6s\,^2S^e_{1/2}$) p-wave threshold yielded EA(Cs)$=0.471\,64(6)$ eV, [STB98] in excellent agreement with the result of Lineberger's group [SRN78, SML85, HL85] quoted in Table 3. The recent work also yielded the first observation of the $Cs^-(6s6p\,^3P^0_1)$ state, appearing as a 5 meV wide resonance centered at 8 meV above the Cs ($6s$) photodetachment threshold [STB98].

5.2. Alkaline Earth Atoms (Be–Ba) and Yb (Z=4, 12, 20, 38, 56, 70)

The discovery of stable negative ions of Ca, Sr, and Ba was one of the (unexpected) highlights in the field of atomic

negative ions since 1985 when it was believed [HL85] that the observed negative ions of the alkaline earth elements should be long-lived excited states. A recent topical review [AAB97] surveys this interesting subfield, and here we present only a brief summary.

The existence of stable Ca^- ions was first demonstrated by Pegg *et al.* [PTC87] in 1987 and theoretically predicted in parallel work by Froese Fischer and co-workers [FLV87]. A surge of theoretical calculations followed (see references in [AAB97]), but it took almost a decade until precise experimental values for the binding energies (see Table 3) of the two stable $ns^2np\ ^2P_J$ fine structure states of $Ca^-(n=4)$, $Sr^-(n=5)$, and $Ba^-(n=6)$ were established by the Aarhus group through laser photodetachment involving s-wave excited state thresholds in combination with state-selective resonance ionization detection (see Sec. 4.2 and [AAB97]). Some of the early theoretical predictions now may appear biased in favor of too large binding energies, but it turned out exceedingly difficult to properly include all relevant valence shell, valence–core and core–core electron correlation effects (see, e.g., [HLH93, SWL96, AB97]). For the Sr^- ion, the binding energies and fine structure splitting were first determined by a combination of accelerator mass spectrometry and laser spectroscopy [BBG95], but subsequently much more accurate values were obtained using LPT with resonant ionization detection [APK97]; the uncertainties were thus reduced by about a factor of 100. The negative barium ion surprised researchers by possessing an extremely long-lived metastable $Ba^-(5d6s6p\ ^4F_{9/2})$ state with a lifetime in the ms region [PVB95, AAB97]; a precise value for its lifetime is, however, not available yet.

To zeroth order, the electron affinities of the alkaline–earth atoms are found to scale linearly with the static atomic polarizability α; for the binding energies of the $^2P_{1/2}$ ground state negative ions of Ca, Sr, and Ba one finds the relation [Ho98]

$$\mathrm{EA}(^2P_{1/2}) = b(\alpha - \alpha_0), \tag{5.2}$$

with $b = 8\times10^{27}\,\mathrm{eV\,m^{-3}}$ and $\alpha_0 = 20.5\times10^{-30}\ \mathrm{m^3}$. From this relation a binding energy of 142 meV is predicted for $Ra^-(^2P_{1/2})$ (using $\alpha(\mathrm{Ra}) = 38.3\times10^{-30}\,\mathrm{m^3}$ [CRC95]). Moreover, the Yb^- ion ($\alpha(\mathrm{Yb}) \approx 21\times10^{-30}\ \mathrm{m^3}$ [CRC95, HD96]) may be not bound in contrast to reports, based on AMS observations [LKG91], that Yb^- is stable with an EA(Yb)>10 meV. A careful search for Yb^- ions by the Aarhus group came to the conclusion [AAP98] that—if stable Yb^- ions exist—the EA of Yb must be smaller than 3 meV. This conclusion agrees with recent findings that no Yb^- ions are formed in collisions of Yb atoms with Rydberg atoms for principal quantum numbers up to 30, suggesting that EA(Yb)<2 meV [RRH98]. In an all-order relativistic many-body calculation for the binding energies in Ca^-, Sr^-, Ba^-, and Yb^-, which yielded close agreement with the experimental values for the alkaline earth ions, Yb^- is predicted to be "slightly unbound," but a positive EA (up to 10 meV) could not be ruled out [AB97]. In a recent many-body theory calculation with scaled electron–atom correlation potential it is predicted that $Yb^-(6s^26p\ ^2P_{1/2})$ represents a narrow shape resonance at 20 meV [DG98].

The addition of an electron to the ground states of Be and Mg atoms does not form stable negative ions. Substantial progress has been recently made, both theoretically and experimentally, with regard to the level structure and lifetimes of long-lived excited Be^- and Mg^- ions [AAB97]. Using the ASTRID storage ring, Balling *et al.* [BAA92] determined the lifetime of a metastable Be^- state as $(45\pm5)\ \mu$s; on the basis of theoretical calculations this state was identified as $Be^-(2s2p^2\ ^4P_{3/2})$. Subsequent state-selective two-photon detachment studies of long-lived Be^- ions, formed by double-electron capture of Be^+ ions in Na vapor, yielded the $Be^-(^4P_J)$ fine structure splittings and the lifetimes of the $J=1/2$ and $J=5/2$ components ($<1\ \mu$s) [ABP96] (see Table 5).

Although the observation of long-lived Mg^- ions has been claimed [BHB66] by mass spectrometry, the nature and existence of such metastable Mg^- ions are uncertain. Theory predicts [Be84] that $Mg^-(3s3p^2\ ^4P_{1/2})$ ions have a lifetime of about 10 μs, but a thorough search for such long-lived Mg^- ions remained unsuccessful [AGS 90], suggesting that any of the $Mg^-(3s3p^2\ ^4P)$ fine structure states must have a lifetime shorter than 1 μs.

5.3. Group III (B–Tl) (Z=5, 13, 31, 49, 81)

Substantial progress has been recently made in theoretical predictions of the EAs of the group III elements, boron through thallium, with uncertainties claimed to be as small as 0.05 eV even for Tl [EIP97] and demonstrated accuracy in the few meV range for B (see Sec. 2 and Table 2). On the experimental side, LPT spectroscopy of the infrared thresholds by Scheer *et al.* has recently yielded precise values for the binding energies and fine-structure splittings of B^- and Al^- with EA(B)=279.723(25) meV [SBH98b] and EA(Al)=432.83(5) meV [SBT98]. We note that the previous LPT result for Al, determined by Calabrese *et al.* [CCT96] through an extrapolated threshold fit as EA(Al)=440.96 (+0.66/−0.48) meV, illustrates the risks when extrapolations are applied over too wide energy ranges without actually observing the relevant threshold.

The good mutual agreement between the three calculations by Arnau *et al.* (configuration interaction plus pseudopotential [AMN92]), Eliav *et al.* (relativistic coupled cluster [EIP97]), and Wijesundera MCDF [Wi97]), for the EAs of B, Al, Ga, and In (see Table 2) and their agreement with the precise LPT values for B and Al [SBT98, SBH98b], and the recent LPES results for In [WCC98b] and Tl [CCT99] demonstrate the progress in the theoretical EA calculations. Conversely, these observations suggest that the LPES result for the EA of Ga [WCC98a] may be somewhat too high. In this context we note that the EA value given in [WCC98a] is uncorrected for the effects of (unresolved) fine structure. An estimate of these effects [Ho 98] suggests that the fine structure-corrected EA is about 0.02 eV lower, i. e., EA(Ga)

TABLE 2. Recent determinations of the electron affinities for the group III atoms (binding energy of $^3P_0$ level in negative ion relative to $^2P_{1/2}$ ground level of atom is given in meV)

	B	Al	Ga	In	Tl
Exp.	279.723(25)[a]	432.83(5)[b]	410(40)[c]	404(9)[d]	377(13)[e]
Theory	279.5(20)[f]	450[g]	290[g]	380[g]	270[g]
	279[h]	427[h]	301[h]	419[h]	400(50)[h,i]
	260[j]	433[j]	305[j]	393[j]	291[j]
	282[k]				

[a](LPT) [SBH98b];
[b](LPT) [SBT98];
[c](LPES) [WCC98a], but value given in this reference (0.43(3)eV) corrected for the effects of fine structure [Ho98];
[d](LPES) [WCC98b];
[e][CCT99];
[f]MCHF with corrections for relativistic, core polarization and core rearrangement effects [FYG95];
[g]MRCI+ pseudopotential [AMN92];
[h](RCC) [EIP97];
[i](RCC) [EKI96];
[j](MCDF) [Wi 97];
[k](r_{12}-MRCI) [Gd 99].

=0.41(4) eV, the value quoted in Table 2 and later in Table 3.

5.4. Group IV (C–Pb) (Z=6, 14, 32, 50, 82)

Systematic studies of the group IV ions: C^-, Si^-, Ge^-, and Sn^- via infrared laser spectroscopy have recently been reported by the McMaster group [TSS96b, SBB98b]. These experiments have led to major improvements (by up to 4 orders of magnitude) in our knowledge of the binding energies of the $^4S_{3/2}$ ground state and of the $^2D_{5/2}$, $^2D_{3/2}$ excited states of these ions (typical uncertainties are 0.2 cm^{-1} except for $C^-(^2D)$). For $C^-(^4S_{3/2})$ the new binding energy of 1.262 118(20) eV [SBB98b] deviates slightly from the previous LPT result 1.2629(3) eV [Fe77]; this difference is attributed to a possible systematic error in the earlier work. The electron affinities of C, Si, Ge, and Sn all fall in the rather narrow range of 1.1–1.4 eV, while for Pb it is much lower (EA(Pb)=0.364(8) eV [FCL81]), mainly due to the influence of the large fine structure splitting in ground state $Pb(^3P)$.

5.5. Group V (N–Bi) (Z=7, 15, 33, 51, 83)

While nitrogen atoms do not form stable negative ions [HL85, CFH97], the heavier group V atoms possess EAs in the range 0.75–1.05 eV with $Sb^-(^3P_2)$ being most strongly bound. A recent LPT study [SHB97] has yielded accurate binding energies for the four bound states of $Sb^-(^3P_{2,1,0}$ and $^1D_2)$; they range from 1.047 40(2) eV ($^3P_2$) to 0.130 84(2) eV ($^1D_2$) [SHB97], (see Tables 3 and 4 in Secs. 6 and 7); in this work, the broadening of transitions by hyperfine structure has been observed. Moreover, infrared LPT spectroscopy yielded an accurate EA for Bi (0.942 363(25) eV [Sc98, Bi99]). Improved values for the EA of As [LXL98] and the fine structure splittings in $As^-(^3P)$ [HLK97] were determined by LPES (see Tables 3 and 4 in Secs. 6 and 7). Otherwise the binding energies and fine structure splittings cited in the 1985 review [HL85] are still valid.

5.6. Group VI (O–Po) (Z=8, 16, 34, 52, 84)

The EAs of the group VI elements, oxygen through polonium, fall in the range of 1.461 eV (oxygen) to 2.077 eV (sulfur). Apart from that of Po, for which no EA measurements have been carried out to our knowledge, the EAs are accurately known from LPT spectroscopy with negative ions in collinear or crossed beams and in traps. As described in earlier sections, nonlinear laser spectroscopic techniques have resulted in improved values for the fine structure splittings in Se^- and Te^-

The EA of oxygen, reported earlier as EA(^{16}O)=11 784.645 cm^{-1} to within 0.006 cm^{-1} (relative uncertainty 5×10^{-7}) [NLA85], quoted as such in [HL85] and later corrected to 11 784.648(6) cm^{-1} in [Bl95] by proper evaluation of the Doppler-shifted thresholds, appears to represent the most accurate experimental determination of a negative ion binding energy. We note, however, that the energy values E_p, E_a for the (Doppler shifted) thresholds with parallel and antiparallel laser and ion beams, extracted from Fig. 3 of [HL85] and from Fig. 2 of [NLA85] as E_p =11 792.405 cm^{-1} and E_a=11 776.950 cm^{-1}, are not compatible with the numbers quoted in the text of [NLA85] (E_p=11 792.376(6) cm^{-1}, E_a=11 776.925(6) cm^{-1}). This incompatibility was not addressed in [NLA85], and it could be simply due to an unmentioned recalibration of the respective photon energy scales. The difference turned into a problem, however, when a recent LPM study of the $^{16}O^-$ ion [VBD99] yielded a somewhat higher result for EA(^{16}O)=11 784.682(21) cm^{-1}; this value was later refined to 11 784.680(15) cm^{-1} [Bl99]. Note that the EA(^{16}O) value, calculated from the two threshold energies read from Fig. 2 of [HL85], is 11 784.675(6) cm^{-1} in close agreement with the LPM result. Although the systematic uncertainties of EA values determined by LPM may need further studies, it is important to note that a recent redetermination of EA(^{19}F) by LPM yielded excellent agreement (to within 0.011 cm^{-1}) [Bl99] with the accurate value (uncertainty 0.025 cm^{-1}) established some time ago by LPT [BCD89] (see Sec. 5.7 and Table 3). We therefore see no obvious reason for the discrepancy between the LPT value [NLA85] and the recent LPM result [VBD99, Bl99] for the EA of the ^{16}O atom, but we have to state that the shift of the threshold energies, imposed on the published experimental spectra in [NLA85], may in fact have been inappropriate. In view of the unresolved situation and for the lack of better knowledge, we quote as the recommended value EA(^{16}O)=11 784.664(22) cm^{-1}, i.e., the average of the two values obtained by Neumark *et al.* [NLA85] and by Blondel *et al.* [VBD99, Bl99] with a suitably chosen error bar.

With regard to the O^- fine structure splitting, the situation is also not fully satisfactory: the value 177.08(5) cm^{-1}, cited in the 1985 review as due to Neumark *et al.*, differs from the

result 177.13(5) cm^{-1} later published by these authors [NLA85]. The recent LPM study of the $^{16}O^-$ ion [VBD99] yielded a fine structure splitting of 177.085(27) cm^{-1}. In Table 4 we recommend the weighted average 177.10(4) cm^{-1} of the values reported in [NLA85] and [VBD99].

In conclusion of this subsection we mention that the LPM study of the negative oxygen ion [VBD99] revealed an interesting isotope shift: in contrast to expectations based on the normal mass shift, the EA for ^{18}O was found to be 0.070 cm^{-1} lower than that for ^{16}O.

5.7. Group VII (F–At) (Z=9, 17, 35, 53, 85)

The EAs of the group VII elements, fluorine through iodine, range from 3.059 038(10) eV (iodine [HG92]) to 3.612 724(27) eV (chlorine [BGH95]). Since 1985 the uncertainties in their values could be reduced substantially and are now in the range (2–27) μeV [BCD89, HG92, BGH95]. The binding energy for Cl^- changed by −4 meV from the 1985 recommendation in [HL85]. The EA of astatine has yet to be measured.

The influence of hyperfine structure in the neutral halogen atoms on the photodetachment threshold data of the negative halogen ions has been observed and taken into account in the determination of the threshold for the lowest hyperfine level [BCD89, HG92, BGH95]. For chlorine the isotope shift between the electron affinities for ^{35}Cl and ^{37}Cl has been measured [BGH95].

5.8. Rare Gas Atoms (He–Rn) (Z=2, 10, 18, 36, 54, 86)

The closed outer shell of the inert gas atoms is unfavorable for a stable anion and these atoms are generally considered incapable of permanently binding an extra electron. He and Ne may be considered as true closed shell atoms, whereas the heavier elements (Ar–Rn) exhibit different physical properties, such as polarizability or chemical reactivity, which could lead to the assumption that these atoms should be considered as "pseudoclosed" shell atoms. It should, however, be pointed out that even though the polarizabilities [CRC95, Sh97] for Ar–Rn are up to a factor of ten larger than for Ne, the values are still of the same order of magnitude as for Zn, Cd, and Hg, for which no stable negative ion has been observed, and a factor of five smaller than for elements like Ca, which is able to form a stable negative ion, but with a very low binding energy. Theoretical calculations [GWW89, NA91] are unable to support the assumption that a stable negative rare gas ion should exist.

He^- exists as a metastable ($1s2s2p\ ^4P$) ion with a binding energy of 77.516(6) meV [KPP97] with respect to He ($1s2s\ ^3S_1$) for the J=5/2 level. Ar^- exists as a metastable ($3p^54s4p\ ^4S_{3/2}$) ion [BHG88] with a binding energy of 32.5(10) meV [PAA98] with respect to Ar($3p^54s\ ^3P_2$). There is no evidence for long-lived metastable states of Ne^- or Kr^-.

Experimental evidence for the existence of a long-lived Xe^- ion has been reported [HKR89]. The ions were formed by crossing a supersonic nozzle jet containing a mixture of xenon and nitrogen with an electron beam operating at 150 eV. The xenon ions were observed only when nitrogen gas was present. It was assumed that the nitrogen gas acted to slow the secondary electrons to lower energy where electron attachment may be possible. So far it has not been possible to identify the Xe^- state involved. There is no evidence for formation of a long-lived Xe^- ion from double charge exchange of Xe^+ interacting with alkali atoms [BPS85], even though the metastable He^- and Ar^- ions are generated by double charge exchange from their positive ions. Further studies of the Xe^- ion would be valuable, taking into consideration that a negative ion state with sextet spin may be long lived. A possible experiment in this direction could start with doubly-charged $Xe^{++}(^3P)$ ions which are subsequently transformed to $Xe^-(^6L_J)$ negative ions by three consecutive electron capture processes. The efficiency for such a process is expected to be low.

5.9. Z=21–30 Atoms (Sc–Zn)

Electron binding energies for the states of five of the elements in the range Z=21–30 have been very significantly improved since the 1985 review. The negative ions of Cr, Co, Ni, and Cu have been studied by high resolution laser photodetachment threshold spectroscopy [BSH98,SBB98a], and the negative ion of Fe by laser photoelectron spectrometry [LL86]. The uncertainties of the EAs for the former group range from 40 μeV to 0.6 meV, and for Fe^- 3 meV. The improvements over previous measurements on these species are large, ranging from 1 to over 2 orders of magnitude. The experimental accuracies far exceed those of any theoretical estimates.

In addition, a study on the titanium negative ion, using electric field detachment techniques [ISS87], has achieved a level of accuracy for the EA (87(7) meV) comparable to the earlier work (79(14) meV) based on electron spectrometry [FCB81]. In Table 3 we quote the weighted average 84(9) meV of these two values.

The studies on Cr^- and Cu^- are straightforward [BSH98], as there is no fine structure in the ground electronic term. Recent work on Ni^- and Co^- yielded much improved values for fine structure splittings [SBB98a]. The $^3F_4$–$^3F_3$ splitting of Co^- was determined to be 875(15) cm^{-1}, while the $^2D_{5/2}$–$^2D_{3/2}$ splitting in Ni^- was found to be 1485(3) cm^{-1}. Due to the very weak signal, the position of the $^3F_2$ state in Co^- was not determined in the recent LPT study [SBB98a]. Limitations of the LPT approach in the complex systems with a number of levels are largely associated with the large backgrounds which result from overlapping thresholds, particularly where p-wave (or higher l) thresholds are involved. Substantial improvements in the fine structure determinations of Sc^-, Ti^-, V^-, Fe^-, and Co^- might be achieved by some combination of RIS, multiphoton detachment, or

stimulated resonant Raman techniques, which were discussed in Secs. 4.2, 4.3, and 4.4.

5.10. $Z=39-48$ Atoms (Y–Cd)

Since the last review, our knowledge of the elements in the range $Z=39-48$ has been significantly advanced in five cases. The measurements of the EAs of Mo and Ag have been improved via infrared LPT studies [BSH98] to the level of 0.2 meV and 20 μeV, respectively. For these elements, only one level is known to be bound. LPT has also facilitated much improved data on the binding energies of the negative ions of Ru [NBB99], Rh [SBB98a], and Pd [SBB98a]. The present accuracies on these three EAs are 0.25, 0.2, and 0.1 meV, well beyond the capabilities of current theoretical techniques for these systems. An accurate measurement of the $^4F_{9/2}-^4F_{7/2}$ fine structure splitting of Ru^- has been performed recently and published jointly with theoretical values for the $J=9/2-5/2$ and $9/2-3/2$ splittings in this ion [NBB99]. The binding energy of the excited $^2D_{5/2}$ level of Pd^- has been determined by LPT to an accuracy of 0.5 meV. An unsuccessful search was performed for the excited $^2D_{3/2}$ level of Pd^- via a $1+1$ magnetic-dipole-enhanced two-photon detachment process [SBB98a]. While the work is not entirely conclusive, it strongly suggests that this level lies above the detachment limit, as indicated in the earlier review [HL85].

The recent LPT studies are all based on p-wave Wigner threshold measurements. As stated for the elements in the range $Z=21-30$, the photodetachment thresholds for negative ions in the $Z=39-48$ range could be measured with low uncertainties if there was essentially no background (e.g., Ag^-) from detachment of excited states, while species with overlapping thresholds (e.g., Ru^-) are much more difficult to determine at a high level of accuracy. The negative ions in the $Z=39-48$ range can also be studied further via a range of multiphoton techniques, both multistep and nonresonant interactions (Secs. 4.2–4.4). The negative ions of zirconium, niobium, and rhodium are particularly notable cases, where a host of nonlinear optical techniques could be applied to great advantage in determining several of the fine structure levels with a much improved accuracy. The case of (radioactive) technetium remains the most poorly determined in this group, with an EA=0.55(20) eV, determined solely via semiempirical extrapolation.

5.11. $Z=57$, 72–80 Atoms (La, Hf–Hg)

The negative ion of lanthanum has attracted considerable attention in recent years due to the fact that it is a potential case of an atomic negative ion which possesses bound states of both even and odd parities [VLM89]. As it has been recently shown that Cs^- does not possess a bound excited state of opposite parity [STB98], despite several earlier theoretical suggestions that this may be the case, La^- has become a focus of considerable interest. Very recently, the EA of lanthanum was measured using laser photoelectron spectroscopy [CCT98]. The EA of La was determined to be 0.47(2) eV, with an excited state bound by 0.17(2) eV. On the basis of the data, it is possible that other states exist. In the future, it would be very interesting to apply infrared laser photodetachment spectroscopy to La^-, in both a single photon and multiphoton regime, in order to achieve much higher resolution and also to verify the existing interpretation of this complex system.

Relatively few developments have occurred in our understanding of atomic negative ions in the range of $Z=72-80$ since the previous review. The notable exceptions are the determinations of EAs and one fine structure splitting in each of the negative ions of iridium and platinum. The electron affinities of Ir^- and Pt^- have been accurately determined by LPT measurements. In the case of the negative ion of platinum, the three measurements [HL73, TSS96b, GDL93] prior to this year differed by somewhat more than might be expected, although they are consistent within two standard deviations. A very recent remeasurement [BSH99], using improved ion source techniques and a new calibration, has provided a more accurate value of 17140.1(4) cm^{-1}, consistent with the earlier work [TSS96b]. Ir^- and Pt^- provided the first demonstration of the utilization of forbidden transitions in the optical regime for the study of atomic negative ion fine structure [TSS96c]. Specifically, resonantly enhanced two-photon detachment processes (via an $M1$ transition) were employed to determine the $^4F_4-^4F_3$ splitting of Ir^- and the $^2D_{5/2}-^2D_{3/2}$ splitting of Pt^-. Although a $2+1$ stimulated Raman process could not be observed by the authors [TSS96c] in either case, a combination of other evidence, together with the subsequent clearly interpreted cases of magnetic dipole transitions for other species, suggests that the original interpretation is correct. At some point in the future an experiment aimed at a clear verification of the original $M1$ study [TSS96c] would, however, be useful.

A variety of established techniques can be applied to further elucidate the properties of negative ions in this category. Ongoing work [Bi99] on W^- and Os^- using LPT is providing additional information on these species, in particular revealing strong resonance structures. A combination of techniques described in this paper could be usefully applied to the negative ions of Hf, Ta, and Re. In particular, the very existence of Hf^- and Re^- remains to be established. For some of the species in this category, the high selectivity and sensitivity afforded by RIS and laser-based storage ring experiments could be applied to our advantage. The complexity of these systems, the weak binding of some of the species, and the greater chance of molecular ion impurities for heavy masses, indicates that more powerful experimental capabilities would be of value.

5.12. $Z=58-71$ (Lanthanides Ce–Lu)

Knowledge of the EAs of the rare earth atoms is still very limited. Semiempirical extrapolations were already available at the time of the previous review [HL85], indicating that the EA values would be in the range up to 0.5 eV, assuming the extra electron to be a d or an f electron. In recent years, with

the increase of computing power, several calculations have been performed [DB93, DB95a, EKI95, VC93] resulting in lower EA values than previously predicted, but also indicating that the extra bound electron most likely is a $6p$ electron. Only Ce can also attach a $5d$ electron. Experimentally all lanthanide negative ions, except Pm^-, Ho^-, and Er^-, have been reported to exist either as stable or long-lived metastable states [NGZ97]. These studies have been performed at tandem accelerators, equipped with sputter ion sources, allowing proper distinction between the atomic ion and possible molecular contaminants. The AMS observation of the Yb^- ion [LKG91] may, however, be considered erroneous as discussed in Sec. 5.2. For some of the elements, Ce [BGH97], Tm, and Dy [NGZ97], preliminary EA values have been obtained applying either laser photodetachment [BGH97] or electric field detachment techniques [NGZ97] in combination with the tandem accelerators. It is, however, not yet known whether the ions studied are present in their ground state or in some long-lived excited state.

5.13. $Z=90-94$ (Actinides Th–Pu)

Only a few of the actinides ($Z=90-103$) have been studied. On the basis of tandem accelerator studies, stable or long-lived negative ions have been reported to exist in Th, Pa, U, and Pu [ZNG93, BBH94, NGZ97]. Theoretical investigations of Th [DB94], Pa [DB96], and U [DB95b], show that these atoms can bind an extra $7p$ electron and Th also a $6d$ electron, exhibiting properties similar to Ce. The EAs for Th, Pa, and U are predicted to be in the range of 150–300 meV.

6. Recommended Values for Atomic Electron Affinities and for Energies of Bound Excited Terms (Table 3)

Table 3 presents those values of atomic EAs which we recommend as being the most reliable. In each case, we have listed the atomic charge Z, the parent atom state, the relevant negative ion state, the binding energy of the negative ion state in both cm^{-1} and eV units ($1eV \triangleq 8065.544\,77(32)$ cm^{-1} [Ta99]) including the respective uncertainty, the method(s) of determination, and the respective references. If different methods have yielded binding energies of similar accuracy, the listed EA represents either a weighted average or our preferred value. In selected cases, the reported error bars represent our judgement, rather than that in the original reference(s). In two important cases (He, Be) where stable negative ions do not exist, we have listed the respective metastable state with the longest lifetime (these ions are relevant for use in tandem accelerators). For the atoms with $Z=58-71$ no experimental EAs are available yet to our knowledge; some information and references on theoretical work are provided in Sec. 5.12; we also refer the reader to references in [HL85].

TABLE 3. Summary of recommended atomic electron affinities

Z	Atom	Atomic State	Neg. Ion State	EA(cm^{-1})[a]	EA(eV)	Method[c]	Ref.
1	H	$1s\ ^2S_{1/2}(F=0)$	$1s^2\ ^1S_0$	6083.064 145(30)	0.754 203 75(3)	Calc.	Dr99
2	He	$1s^2\ ^1S_0$		<0	<0	Calc.; SE	HL85
		$1s2s\ ^3S_1$	$1s2s2p\ ^4P_{5/2}(m)$	625.21(5)	0.077 516(6)	LPT	KPP97
3	Li	$2s\ ^2S_{1/2}$	$2s^2\ ^1S_0$	4984.90(17)	0.618 049(21)	LPT	HHK96
4	Be	$2s^2\ ^1S_0$		<0	<0	Calc.; SE	HL85
		$2s2p\ ^3P_0$	$2s2p^2\ ^4P_{3/2}(m)$	2344.9(8)	0.290 74(10)	LPT	KPA95
5	B	$2p\ ^2P_{1/2}$	$2p^2\ ^3P_0$	2256.12(20)	0.279 723(25)	LPT	SBH98b
6	C	$2p^3\ ^3P_0$	$2p^3\ ^4S_{3/2}$	10 179.67(15)	1.262 118(20)	LPT	SBB98b
			$2p^3\ ^2D(m)$[b]	266(8)	0.033(1)	LPT	Fe77
7	N	$2p^3\ ^4S_{3/2}$	$2p^4\ ^3P$	−560(160)	−0.07(2)	Diss. Att.	MGH78
8	O	$2p^4\ ^3P_2$	$2p^5\ ^2P_{3/2}$	11 784.664(22)	1.461 112 0(27)	LPT/LPM	NLA85,Bl95/ VBD99,Bl99
9	F	$2p^5\ ^2P_{3/2}$	$2p^6\ ^1S_0$	27 432.440(25)	3.401 188 7(32)	LPT	BCD89
10	Ne	$2p^6\ ^1S_0$		<0	<0	Calc.; SE	HL85
11	Na	$3s\ ^2S_{1/2}$	$3s^2\ ^1S_0$	4419.32(20)	0.547 926(25)	LPT	HL85
12	Mg	$3s^2\ ^1S_0$		<0	<0	Calc.;e^- scatt.	HL85
13	Al	$3p\ ^2P_{1/2}$	$3p^2\ ^3P_0$	3491.0(4)	0.432 83(5)	LPT	SBT98
			$3p^2\ ^1D_2(m)$	880(80)	0.109(10)	LPES(O^-)	FCL81
14	Si	$3p^2\ ^3P_0$	$3p^3\ ^4S_{3/2}$	11 207.24(15)	1.389 521(20)	LPT	SBB98b
			$3p^3\ ^2D_{3/2}(m)$	4252.43(20)	0.527 234(25)	LPT	SBB98b
			$3p^3\ ^2P_{1/2}(m)$	230(40)	0.029(5)	LPES(K^-)	KHL75
15	P	$3p^3\ ^4S_{3/2}$	$3p^4\ ^3P_2$	6021(3)	0.7465(3)	LPT	Fe76/SL77
16	S	$3p^4\ ^3P_2$	$3p^5\ ^2P_{3/2}$	16 752.966(8)	2.077 102 9(10)	LPT	LS85/HL85
17	Cl	$3p^5\ ^2P_{3/2}$	$3p^6\ ^1S_0$	29 138.59(22)	3.612 724(27)	LPT	BGH95
18	Ar	$3p^6\ ^1S_0$		<0	<0	Calc.; SE	HL85
19	K	$4s\ ^2S_{1/2}$	$4s^2\ ^1S_0$	4044.54(10)	0.501 459(12)	LPT	ASK99
20	Ca	$4s^2\ ^1S_0$	$4s^24p\ ^2P_{1/2}$	198.0(8)	0.02455(10)	LPT	PAB96
21	Sc	$3d4s^2\ ^2D_{3/2}$	$3d4s^24p\ ^{1,3}D$	1520(160)	0.188(20)	LPES(O^-)	FHL81
			$3d4s^24p\ ^{3,1}D(m)$	330(160)	0.041(20)	LPES(O^-)	FHL81
22	Ti	$3d^24s^2\ ^3F_2$	$3d^34s^2\ ^4F_{3/2}$	680(70)	0.084(9)	LPES(O^-)/FD	FCB81/ISS87
23	V	$3d^34s\ 4^5_{3/2}$	$3d^44s^2\ ^5D_0$	4230(100)	0.525(12)	LPES(O^-)	FCB81

TABLE 3. Summary of recommended atomic electron affinities—Continued

Z	Atom	Atomic State	Neg. Ion State	EA(cm^{-1})[a]	EA(eV)	Method[c]	Ref.
24	Cr	$3d^5 4s\ ^7S_3$	$3d^5 4s^2\ ^6S_{5/2}$	5451.0(10)	0.675 84(12)	LPT	BSH98
25	Mn	$3d^5 4s^2\ ^6S_{5/2}$		<0	<0	SE; calc.	HL85
26	Fe	$3d^6 4s^2\ ^5D_4$	$3d^7 4s^2\ ^4F_{9/2}$	1220(25)	0.151(3)	LPES(O^-)	LL86
27	Co	$3d^7 4s^2\ ^4F_{9/2}$	$3d^8 4s^2\ ^3F_4$	5350(5)	0.6633(6)	LPT	SBB98a
28	Ni	$3d^8 4s^2\ ^3F_4$	$3d^9 4s^2\ ^2D_{5/2}$	9333.1(10)	1.15716(12)	LPT	SBB98a
29	Cu	$3d^{10} 4s\ ^2S_{1/2}$	$3d^{10} 4s^2\ ^1S_0$	9967.2(3)	1.23578(4)	LPT	BSH98
30	Zn	$4s^2\ ^1S_0$		<0	<0	e^- scatt.; SE	HL85
31	Ga	$4p\ ^2P_{1/2}$	$4p^2\ ^3P_0$	3300(300)	0.41(4)	LPES(O^-,Cu^-)	WCC98a,Ho98
32	Ge	$4p^2\ ^3P_0$	$4p^3\ ^4S_{3/2}$	9942.49(12)	1.232 712(15)	LPT	SBB98b
			$4p^3\ ^2D_{3/2}(m)$	3237.9(8)	0.401 44(10)	LPT	SBB98b
33	As	$4p^3\ ^4S_{3/2}$	$4p^4\ ^3P_2$	6570(70)	0.814(8)	LPES(O^-,NO^-)	LXL98
34	Se	$4p^4\ ^3P_2$	$4p^5\ ^2P_{3/2}$	16 297.8(2)	2.020 67(2)	LPT	MEL88
35	Br	$4p^5\ ^2P_{3/2}$	$4p^6\ ^1S_0$	27 129.170(15)	3.363 588 0(20)	LPT	BCD89
36	Kr	$4p^6\ ^1S_0$		<0	<0	SE	HL85
37	Rb	$5s\ ^2S_{1/2}$	$5s^2\ ^1S_0$	3919.18(15)	0.485 916(20)	LPT	FBH78
38	Sr	$5s^2\ ^1S_0$	$5s^2 5p\ ^2P_{1/2}$	419.9(5)	0.052 06(6)	LPT	APK97
39	Y	$4d5s^2\ ^2D_{3/2}$	$4d5s^2 5p\ ^1D_2$	2480(100)	0.307(12)	LPES(O^-)	FHL81
			$4d5s^2 5p\ ^3D_1(m)$	1320(200)	0.164(25)	LPES(O^-)	FHL81
40	Zr	$4d^2 5s^2\ ^3F_2$	$4d^3 5s^2\ ^4F_{3/2}$	3440(110)	0.426(14)	LPES(O^-)	FCB81
41	Nb	$4d^4 5s\ ^6D_{1/2}$	$4d^4 5s^2\ ^5D_0$	7200(200)	0.893(25)	LPES(O^-)	FCB81
42	Mo	$4d^5 5s\ ^7S_3$	$d^5 5s^2\ ^6S_{5/2}$	6027(2)	0.7472(2)	LPT	BSH98
43	Tc	$4d^5 5s^2\ ^6S_{5/2}$	$4d^6 5s^2\ ^5D_4$	4400(1600)	0.55(20)	SE	FCB81
44	Ru	$4d^7 5s\ ^5F_5$	$4d^7 5s^2\ ^4F_{9/2}$	8439.6(20)	1.046 38(25)	LPT	NBB99
45	Rh	$4d^8 5s\ ^4F_{9/2}$	$4d^8 5s^2\ ^3F_4$	9218.0(15)	1.142 89(20)	LPT	SBB98a
46	Pd	$4d^{10}\ ^1S_0$	$4d^{10} 5s\ ^2S_{1/2}$	4534.0(10)	0.562 14(12)	LPT	SBB98a
			$4d^9 5s^2\ ^2D_{5/2}(m)$	3407(4)	0.4224(5)	LPT	SBB98a
47	Ag	$4d^{10} 5s\ ^2S_{1/2}$	$4d^{10} 5s^2\ ^1S_0$	10521.3(2)	1.30447(2)	LPT	BSH98
48	Cd	$4d^{10} 5s^2\ ^1S_0$		<0	<0	e^- scatt.; SE	HL85
49	In	$5p\ ^2P_{1/2}$	$5p^2\ ^3P_0$	3260(70)	0.404(9)	LPES(Na^-)	WCC98b
50	Sn	$5p^2\ ^3P_0$	$5p^3\ ^4S_{3/2}$	8969.42(12)	1.112 066(15)	LPT	SBB98b
			$5p^3\ ^2D_{3/2}(m)$	3207.00(12)	0.397 617(15)	LPT	SBB98b
51	Sb	$5p^3\ ^4S_{3/2}$	$5p^4\ ^3P_2$	8447.86(15)	1.047 401(20)	LPT	SHB97
			$5p^4\ ^1D_2$	1055.3(2)	0.130 84(2)	LPT	SHB97
52	Te	$5p^4\ ^3P_2$	$5p^5\ ^2P_{3/2}$	15 896.18(5)	1.970 875(7)	LPT	HKR96
53	I	$5p^5\ ^2P_{3/2}$	$5p^6\ ^1S_0$	24 672.81(8)	3.059 038(10)	LPT	HG92
54	Xe	$5p^6\ ^1S_0$		< 0	<0	SE	HL85
55	Cs	$6s\ ^2S_{1/2}$	$6s^2\ ^1S_0$	3803.92(20)	0.471 626(25)	LPT	SRN78/SML85;HI85/STB98
56	Ba	$6s^2\ ^1S_0$	$6s^2 6p^2P_{1/2}$	1166.4(5)	0.144 62(6)	LPT	PVB95
57	La	$5d6s^2\ ^2D_{3/2}$	$5d^2 6s^2\ ^3F_2$	3790(160)	0.47(2)	LPES	CCT98
58	Rare earths			<4000	<0.5	semiempirical estimates	
71							
72	Hf	$5d^2 6s^2\ ^3F_2$	$5d^3 6s^2\ ^4F$	≅ 0	≅ 0	SE	HL85
73	Ta	$5d^3 6s^2\ ^4F_{3/2}$	$5d^4 6s^2\ ^5D_0$	2600(100)	0.322(12)	LPES(O^-)	FCB81
74	W	$5d^4 6s^2\ ^5D_0$	$5d^5 6s^2\ ^6S_{5/2}$	6570(60)	0.815(8)	LPES(O^-)	FCB81
75	Re	$5d^5 6s^2\ ^6S_{5/2}$	$5d^6 6s^2\ ^5D_4$	1200(1200)	0.15(15)	SE; SSI	FCB81
76	Os	$5d^6 6s^2\ ^5D_4$	$5d^7 6s^2\ ^4F_{9/2}$	8693(1)	1.077 80(12)	LPT	Bi99
77	Ir	$5d^7 6s^2\ ^4F_{9/2}$	$5d^8 6s^2\ ^3F_4$	12617.4(12)	1.564 36(15)	LPT	BSH99
78	Pt	$5d^9 6s^3D_3$	$5d^9 6s^2\ ^2D_{5/2}$	17140.1(4)	2.125 10(5)	LPT	BSH99
79	Au	$5d^{10} 6s\ ^3S_{1/2}$	$5d^{10} 6s^2\ ^1S_0$	18620.2(2)	2.308 61(3)	LPT	HL73/HL85
80	Hg	$6s^2\ ^1S_0$		<0	<0	e^- scatt.; SE	HL85
81	Tl	$6s^2 6p\ ^2P_{1/2}$	$6p^2\ ^3P_0$	3040(100)	0.377(13)	LPES(Na^-)	CCT99
82	Pb	$6p^2\ ^3P_0$	$6p^3\ ^4S_{3/2}$	2940(60)	0.364(8)	LPES(O^-)	FCL81
83	Bi	$6p^3\ ^4S_{3/2}$	$6p^4\ ^3P_2$	7600.68(20)	0.942 363(25)	LPT	Sc98,Bi99
84	Po	$6p^4\ ^3P_2$	$6p^5\ ^2P_{3/2}$	15300(2400)	1.9(3)	SE	HL85
85	At	$6p^5\ ^2P_{3/2}$	$6p^2\ ^1S_0$	22600(1600)	2.8(2)	SE	HL85
86	Rn	$6p^6\ ^1S_0$		<0	<0	SE	HL85

[a]Conversion factor from eV to cm^{-1}: 1.239 841 857(49)×10^{-4} eV/cm^{-1} [Ta99]. For electron affinities reported in eV only, we have converted the EA values to cm^{-1} by rounding off according to the level of uncertainty.

[b](m) indicates metastable.

[c]Abbreviations used: (Calc.) *ab initio* calculations; (LPT) tunable laser photodetachment threshold; (LPES) laser photodetachment electron spectrometry; (LPM) laser photodetachment microscopy; (SE) semiempirical extrapolation (isoelectronic extrapolation and/or horizontal analysis); (SSI) self-surface ionization; (e^- scatt) electron scattering resonance; (Diss.Att.) dissociative attachment of electrons; (FD) field detachment.

7. Recommended Values for Fine Structure Splittings in Negative Ions (Table 4)

Table 4 presents recommended values for the fine structure splittings in atomic negative ions. The splittings are found to be systematically smaller than the fine structure intervals in the respective isoelectronic neutral atoms; this reflects the more diffuse nature of the relevant open shell orbitals in the negative ions, resulting—in conjunction with the difference between the $(1/r)dV/dr$ functions ($V(r)$ = potential energy)—in smaller spin-orbit parameters.

TABLE 4. Fine structure splittings in atomic negative ions

Z	Ion	J–J′ [a]	Splitting (cm^{-1})	Method [b]	Reference
2	$He^-(^4P)$	5/2 → 3/2	0.027 508(27)	rf-sp.	MN73
		5/2 → 1/2	0.2888(18)	rf-sp.	MN73
4	$Be^-(^4P)$	1/2 → 3/2	0.74(7)	LPT	ABP96
		3/2 → 5/2	0.59(7)	LPT	ABP96
5	$B^-(^3P)$	0 → 1	3.23(15)	LPT	SBH98b
		1 → 2	5.18(15)	LPT	SBH98b
		0 → 2	8.41(20)	LPT	SBH98b
6	$C^-(^2D)$	3/2 → 5/2	3(1)	LIE	HL75
8	$O^-(^2P)$	3/2 → 1/2	177.10(4)	LPT/LPM	NLA85/VBD99
13	$Al^-(^3P)$	0 → 1	22.7(3)	LPT	SBT98
		1 → 2	45.7(2)	LPT	SBT98
14	$Si^-(^2D)$	3/2 → 5/2	14.08(20)	LPT	SBB98b
15	$P^-(^3P)$	2 → 1	181(2)	LPT	Fe76; SL77
		2 → 0	263(2)	LPT	Fe76: SL77
16	$S^-(^2P)$	3/2 → 1/2	483.54(1)	LPT	HL85
20	$Ca^-(^2P)$	1/2 → 3/2	39.24(11)	LPT	KBP97
22	$Ti^-(^4F)$	3/2 → 5/2	72(7)	LIE	FCB81
		5/2 → 7/2	99(10)	LIE	FCB81
		7/2 → 9/2	124(12)	LIE	FCB81
		3/2 → 9/2	295(15)	LIE	FCB81
23	$V^-(^5D)$	0 → 1	35(4)	RIE	FCB81
		1 → 2	70(7)	RIE	FCB81
		2 → 3	100(10)	RIE	FCB81
		3 → 4	125(13)	RIE	FCB81
		0 → 4	330(17)	RIE	FCB81
26	$Fe^-(^4F)$	9/2 → 7/2	540(50)	RIE	FCB81
		7/2 → 5/2	390(40)	RIE	FCB81
		5/2 → 3/2	270(30)	RIE	FCB81
		9/2 → 3/2	1200(60)	RIE	FCB81
27	$Co^-(^3F)$	4 → 3	875(15)	LPT	SBB98a
		3 → 2	650(50)	LPES	CEL79
		4 → 2	1560(50)	LPES	CEL79
28	$Ni^-(^2D)$	5/2 → 3/2	1485(3)	LPT	SBB98a
31	$Ga^-(^3P)$	0 → 1	220(20)	RIE; QIE	HL75; 85
		0 → 2	580(50)	RIE; QIE	HL75; 85
32	$Ge^-(^2D)$	3/2 → 5/2	192.6(9)	LPT	SBB98b
33	$As^-(^3P)$	2 → 1	1008(25)	LPES	HLK97
		2 → 0	339(40)	LPES	HLK97
34	$Se^-(^2P)$	3/2 → 1/2	2278.2(2)	LPT/SRS	TSS96a
38	$Sr^-(^2P)$	1/2 → 3/2	160.4(3)	LPT	KBP97
40	$Zr^-(^4F)$	3/2 → 5/2	250(50)	RIE	FCB81
		5/2 → 7/2	330(70)	RIE	FCB81
		7/2 → 9/2	370(70)	RIE	FCB81
		3/2 → 9/2	950(100)	RIE	FCB81
41	$Nb^-(^5D)$	0 → 1	110(20)	RIE	FCB81
		1 → 2	200(40)	RIE	FCB81
		2 → 3	250(40)	RIE	FCB81
		3 → 4	310(60)	RIE	FCB81
		0 → 4	860(90)	RIE	FCB81
44	$Ru^-(^4F)$	9/2 → 7/2	1461(9)	LPT	NBB99
		9/2 → 5/2	2266	Theory	NBB99
		9/2 → 3/2	2831	Theory	NBB99
45	$Rh^-(^3F)$	4 → 3	2370(65)	LPES	FCB81
		3 → 2	1000(65)	LPES	FCB81
		4 → 2	3370(65)	LPES	FCB81

TABLE 4. Fine structure splittings in atomic negative ions—Continued

Z	Ion	J–J′ [a]	Splitting (cm^{-1})	Method [b]	Reference
46	$Pd^-(^2D)$	5/2 → 3/2 [c]	3450(350)	RIE	FCB81
49	$In^-(^3P)$	0 → 1	680(70)	RIE; QIE	HL75; 85
		0 → 2	1550(150)	RIE; QIE	HL75; 85
50	$Sn^-(^2D)$	3/2 → 5/2	749.95(15)	LPT	SBB98b
51	$Sb^-(^3P)$	2 → 1	2684.37(15)	LPT	SHB97
		2 → 0	2800.8(6)	LPT	SHB97
52	$Te^-(^2P)$	3/2 → $\frac{1}{2}$	5005.36(10)	SRS	SBH98a
56	$Ba^-(^2P)$	1/2 → 3/2	443.8(7)	LPT	PVB95
73	$Ta^-(^5D)$	0 → 1	1070(110)	LPES	FCB81
		1 → 2	1170(120)	LPES	FCB81
76	$Os^-(^4F)$	9/2 → 7/2	4231(25)	LPT	Bi99
77	$Ir^-(^4F)$	4 → 3	7087.3(4)	RDS	TSS96c
78	$Pt^-(^2D)$	5/2 → 3/2	9740.9(5)	RDS	TSS96c

[a]Total angular momenta of lower (left) and upper fine structure levels are listed.
[b]Abbreviations used: (rf) radio frequency techniques; (RIE) isoelectronic extrapolation of ratios of fine structure separations; (LIE) isoelectronic extrapolation from a logarithmic plot; (QIE) quadratic isoelectronic extrapolation; (LPT) tunable laser photodetachment threshold; (LPES) laser photodetachment electron spectrometry; (LPM) laser photodetachment microscopy; (RDS) resonant multiphoton detachment spectroscopy; (SRS) stimulated Raman scattering detachment spectroscopy.
[c]$J = 3/2$ not bound.

8. Experimental Lifetimes of Long-Lived Excited States of Negative Ions (Table 5)

TABLE 5. Experimental lifetimes of long-lived excited states of negative ions

Z	Ion	J	Lifetime (μs)	References
2	$He^-(1s2s2p\ ^4P)$	5/2	345(10)[a]	AAB93, WBB99
		3/2	11(2)[a]	AAB93, NW70, WBB99
		1/2	9(2)[a]	SBG71, WBB99
4	$Be^-(2s2p^2\ ^4P)$	5/2	0.33(6)	ABP96
		3/2	42.07(12)	KBA99
		1/2	0.73(8)	ABP96
18	$Ar^-(3p^54s4p\ ^4S)$	3/2	0.26(3)	BHG88
56	$Ba^-(5d6s6p\ ^4F)$	9/2	~5000	AAB97

[a]Average value of published results.

9. Future Perspectives

In spite of the substantial experimental efforts over the past 14 yrs since the last review [HL85], there still remain a number of outstanding issues regarding the binding energies and excited states of atomic negative ions. The most notable area is that of the rare earths, where knowledge is either completely lacking, or in other cases, largely rather qualitative or semiquantitative in nature. In order to overcome the experimental problems with the rare earth negative ions, it will probably be necessary to apply some combination of techniques. Initial studies using LPES may be of value in order to survey the ionic structural properties, followed by one of the more sensitive and selective techniques, including: RIS, infrared laser spectroscopy, as well as storage ring, trap, and AMS studies. A combination of approaches may frequently be indicated in order to avoid the systematic problems which are associated with these complex, and often weakly bound ions. It could also be valuable to have a few highly accurate experiments conducted on very heavy ions such as Re^-, Th^-, and U^-, which would allow a calibration of extrapolation techniques, as well as theoretical efforts on these very heavy species. Recent work on a number of atomic species of intermediate and high mass, using infrared and multiphoton techniques, have led to much improved data on the binding energies of a number of species. Nevertheless, infrared laser, multiphoton, and stimulated Raman experiments could still be applied to selected species in order to vastly improve the data in a number of cases. In particular the Raman approach should be tested on a wider range of species than has been done to date. The species of interest include, for example, excited states of some transition metal ions as well as EAs for ions such as Ti^-, Ga^-, As^-, and Tc^-. Finally, a few additional experiments would be welcome on selected light ionic species, in order to provide critical challenges for advanced theoretical techniques. A singularly interesting case is the three-body system represented by the hydrogen negative ion. For H^-, theory clearly exceeds experiment by a very substantial margin in terms of the binding energy determination of the ground electronic state. If an experiment can be designed to equal or exceed theory in accuracy, this would become a very important benchmark in the field. Studies which extend the recent Penning-trap-based investigations [HZG97] experiments on H^- may achieve this goal, but their task appears to be a very challenging one.

Future work could benefit from further developments in experimental techniques. Very narrow linewidth pulsed sources might be employed, either in the form of grazing incidence tunable pulsed lasers or via narrow-band cw-laser injection seeding of a pulsed laser amplifier. This would maintain the advantages of time-gated experiments while extending the resolution to near the Fourier transform limit, in order to further explore fundamental issues in light atomic

species. Both optical parametric oscillators (OPOs), as well as shorter pulse systems, potentially based on mode-locked laser sources operating in the range of a few picoseconds to a few hundred picoseconds, may prove very useful. The OPOs offer very intense light generation in the infrared wavelength regime, allowing extensions of the infrared spectroscopic measurements achieved to date to yet more challenging cases. In cases where nonlinear optical conversion and nonlinear interaction between the laser beam and the ion is required, the shorter pulse systems offer great advantages, provided that the Fourier transform limit does not lead to an unacceptably large laser linewidth. The ever-increasing utilization of solid state technology, both in terms of powerful semiconductor diode arrays and doped dielectric crystals, combined with improved laser engineering, make higher repetition rate lasers much more feasible. Laser systems operating in the repetition rate range of 100 Hz–1 kHz, for example, will facilitate many experiments which could not be conducted with the 10 Hz Nd:YAG-pumped dye laser systems which have formed the basis of the recent resonant multiphoton experiments. Ion beam techniques too will benefit from technical advances. State-selective ion beam production techniques could be used to populate specific ionic levels of interest, or to effectively form very weakly bound species. Also, combinations of tunable laser and electron spectroscopic approaches may prove effective in the study of complex weakly bound systems. In addition, rf-optical experiments might be designed to address fine structure or hyperfine structure measurements. Storage ring techniques, which have proven particularly useful in the study of metastable atomic negative ions, could play an important role in sorting out a number of the remaining issues regarding the energies of bound states. Finally, combinations of laser and electron spectroscopic methods may prove effective in the study of complex bound systems; in particular, photodetachment microscopy [BDD96, VBD99] and related techniques may become important in the next few years.

10. Note Added in Proof

After submission of this article results of a benchmark *ab initio* and density-functional theory study, which included scalar relativistic and spin-orbit coupling effects, have been published for the electron affinities of the first- and second-row atoms [G. de Oliveira, J. M. L. Martin, F. de Proft, and P. Geerlings, Phys. Rev. A **60** 1034 (1999)]. On average, the best *ab initio* results agreed to about 1 meV or better with the most recent experimental results. Accurate theoretical predictions of electron affinities, which have not yet been determined otherwise, are of obvious interest.

11. Acknowledgments

It is our pleasure to acknowledge W. Carl Lineberger for many fruitful interactions regarding negative ion spectroscopy and for his long-standing efforts to promote the knowledge of binding energies in atomic and molecular negative ions. We gratefully acknowledge R. C. Bilodeau, C. Blonde G. W. F. Drake, D. Hanstorp, B. N. Taylor, and J. S Thompson for providing results prior to publication and fc helpful discussions, and we thank M. Scheer for comment on this article. We acknowledge G. Koschmann and S. Tolc for secretarial help with the manuscript. H. Haugen and I Hotop thank the Aarhus Center for Atomic Physics for sup port of a visit to Aarhus during which part of the work o this article was carried out.

12. References

AAB93 T. Andersen, L. H. Andersen, P. Balling, H. K Haugen, P. Hvelplund, W. W. Smith, and K Taulbjerg, Phys. Rev. A **47**, 890 (1993).

AAB97 T. Andersen, H. H. Andersen, P. Balling, P Kristensen, and V. V. Petrunin, J. Phys. B **30** 3317 (1997).

AAH97 L. H. Andersen, T. Andersen, and P. Hvelplund Adv. At. Mol. Opt. Phys. **38**, 155 (1997).

AAP98 H. H. Andersen, T. Andersen, and U. V. Peder sen, J. Phys. B **31**, 2239 (1998).

AB97 E. N. Avgoustoglou and D. R. Beck, Phys. Rev A **55**, 4143 (1997).

ABP96 H. H. Andersen, P. Balling, V. V. Petrunin, an T. Andersen, J. Phys. B **29**, L415 (1996).

AGS90 T. Andersen, J. O. Gaardsted, L. Eg Sørensen and T. Brage, Phys. Rev. A **42**, 2728 (1990).

AKL91 S. A. Aseyev, Yu. A. Kudryavtsev, V. S Lethokov, and V. V. Petrunin, Opt. Lett. **16**, 51 (1991).

AMN92 F. Arnau, F. Mota, and J. J. Novoa, Chem. Phys **166**, 77 (1992).

An97 T. Andersen, Nucl. Instrum. Methods Phys. Res B **123**, 508 (1997).

APK97 H. H. Andersen, V. V. Petrunin, P. Kristensen and T. Andersen, Phys. Rev. A **55**, 3247 (1997)

ASK99 K. T. Andersson, J. Sandstrom, I. Yu. Kiyan, D Hanstorp, and D. J. Pegg, Phys. Rev. A (submitted); D. Hanstorp (private communication 1999).

Ba91 D. R. Bates, Adv. At. Mol. Opt. Phys. **27**, 1 (1991).

BAA92 P. Balling, L. H. Andersen, T. Andersen, H. K Haugen, P. Hvelplund, and K. Taulbjerg, Phys Rev. Lett. **69**, 1042 (1992).

BBG95 D. Berkovits, E. Boaretto, S. Ghelberg, O. Heber, and M. Paul, Phys. Rev. Lett. **75**, 414 (1995).

BBH94 D. Berkovits, E. Boaretto, O. Heber, G. Hollos G. Korschinek, W. Kutschera, and M. Paul Nucl. Instrum. Methods Phys. Res. B **92**, 254 (1994).

BBS90 B. Barbieri, N. Beverini, and A. Sasso, Rev Mod. Phys. **62**, 603 (1990).

BC94 S. J. Buckman and C. W. Clark, Rev. Mod. Phys **66**, 539 (1994).

BCD89 C. Blondel, P. Cacciani, C. Delsart, and R. Trainham, Phys. Rev. A **40**, 3698 (1989).

BCD91 C. Blondel, M. Crance, C. Delsart, and A. Giraud, J. Phys. B **24**, 3575 (1991).

BD86 W. K. Bischel and M. J. Dyer, Phys. Rev. A **33**, 3113 (1986).

BDD96 C. Blondel, C. Delsart, and F. Dulieu, Phys. Rev. Lett. **77**, 3755 (1996).

BDD99 C. Blondel, C. Delsart, F. Dulieu, and C. Valli, Eur. Phys. J. D **5**, 207 (1999).

Be84 D. R. Beck, Phys. Rev. A **30**, 3305 (1984).

BGH95 U. Berzinsh, M. Gustafsson, D. Hanstorp, A. Klinkmüller, U. Ljungblad, and A.-M. Mårtensson-Pendrill, Phys. Rev. A **51**, 231 (1995).

BGH97 D. Berkovits, S. Ghelberg, O. Heber, and M. Paul, Nucl. Instrum. Methods Phys. Res. B **123**, 515 (1997).

BHB66 K. Bethge, E. Heinicke, and H. Baumann, Phys. Lett. **23**, 542 (1966).

BHG88 I. Ben-Itzhak, O. Heber, I. Gertner, and B. Rosner, Phys. Rev. A **38**, 4870 (1988).

Bi99 R. Bilodeau (private communication, 1999).

Bl95 C. Blondel, Physi. Scr. T **58**, 31 (1995).

Bl99 C. Blondel (private communication, 1999).

BNW70 L. M. Blau, R. Novick, and D. Weinflash, Phys. Rev. Lett. **24**, 1268 (1970).

Bö98 G. Bönsch, Metrologia **35**, 133 (1998).

BPS85 Y. K. Bae, J. R. Peterson, A. J. Schlachter, and J. W. Stearns, Phys. Rev. Lett. **54**, 789 (1985).

BSH98 R. C. Bilodeau, M. Scheer, and H. K. Haugen, J. Phys. B **31**, 3885 (1998).

BSH99 R. C. Bilodeau, M. Scheer, H. K. Haugen, and R. L. Brooks, Phys. Rev. A (submitted, 1999).

Bu86 A. V. Bunge, Phys. Rev. A **33**, 82 (1986).

BZY95 E. de Beer, Y. Zhao, I. Yourshaw, and D. M. Neumark, Chem. Phys. Lett. **244**, 400 (1995).

CB96 A. W. Castleman, Jr. and K. H. Bowen, Jr., J. Phys. Chem. **100**, 12911 (1996).

CCT96 D. Calabrese, A. M. Covington, J. S. Thompson, R. W. Marawar, and J. W. Farley, Phys. Rev. A **54**, 2797 (1996).

CCT98 A. M. Covington, D. Calabrese, J. S. Thompson, and T. J. Kvale, J. Phys. B **31**, L855 (1998).

CCT99 D. L. Carpenter, A. M. Covington, and J. S. Thompson, Phys. Rev. A (accepted); J. S. Thompson, private communication (1999).

CEL79 R. R. Corderman, P. C. Engelking, and W. C. Lineberger, J. Chem. Phys. **70**, 4474 (1979).

CFH97 R. D. Cowan, C. Froese Fischer, J. E. Hansen, and V. Kempter, J. Phys. B **30**, 1457 (1997).

Ch97 K. T. Chung (private communication, 1997).

CKR63 S. B. Crampton, D. Kleppner, and N. F. Ramsey, Phys. Rev. Lett. **11**, 338 (1963).

CRC95 *CRC Handbook of Chemistry and Physics*, edited by D. R. Lide (CRC, Boca Raton, FL, 1995).

DB93 D. Datta and D. R. Beck, Phys. Rev. A **47**, 5198 (1993).

DB94 D. Datta and D. R. Beck, Phys. Rev. A **50**, 1107 (1994).

DB95a K. Dinov and D. R. Beck, Phys. Rev. A **51**, 1680 (1995).

DB95b K. D. Dinov and D. R. Beck, Phys. Rev. A **52**, 2632 (1995).

DB96 K. D. Dinov and D. R. Beck, Phys. Rev. A **53**, 4031 (1996).

DG98 V. A. Dzuba and G. F. Gribakin, J. Phys. B **31**, L483 (1998).

DM98 G. W. F. Drake and W. C. Martin, Can. J. Phys. **76**, 679 (1998).

DMH91 M. D. Davidson, H. G. Muller, and H. B. van Linden van den Heuvell, Phys. Rev. Lett. **67**, 1712 (1991).

Dr88 G. W. F. Drake, Nucl. Instrum. Methods Phys. Res. B **31**, 7 (1988).

Dr99 G. W. F. Drake (private communication, 1999).

EHL88 K. M. Ervin, J. Ho, and W. C. Lineberger, J. Phys. Chem. **92**, 5405 (1988).

EIP97 E. Eliav, Y. Ishikawa, P. Pyykkö, and U. Kaldor, Phys. Rev. A **56**, 4532 (1997).

EKI95 E. Eliav, U. Kaldor, and Y. Ishikawa, Phys. Rev. A **52**, 291 (1995).

EKI96 E. Eliav, U. Kaldor, Y. Ishikawa, M. Seth, and P. Pyykkö, Phys. Rev. A **53**, 3926 (1996).

Fa89 J. W. Farley, Phys. Rev. A **40**, 6286 (1989).

FBH78 P. Frey, F. Breyer, and H. Hotop, J. Phys. B **11**, L589 (1978).

FCB81 C. S. Feigerle, R. R. Corderman, S. V. Bobashev, and W. C. Lineberger, J. Chem. Phys. **74**, 1580 (1981).

FCL81 C. S. Feigerle, R. R. Corderman, and W. C. Lineberger, J. Chem. Phys. **74**, 1513 (1981).

Fe76 D. Feldmann, Z. Phys. A **277**, 19 (1976).

Fe77 D. Feldmann, Chem. Phys. Lett. **47**, 338 (1977).

FHL81 C. S. Feigerle, Z. Herman, and W. C. Lineberger, J. Electron Spectrosc. Relat. Phenom. **23**, 441 (1981).

Fi93 C. Froese Fischer, J. Phys. B **26**, 855 (1993).

FLV87 C. Froese Fischer, J. B. Lagowski, and S. H. Vosko, Phys. Rev. Lett. **59**, 2263 (1987).

FYG95 C. Froese Fischer, A. Ynnerman, and G. Gaigalas, Phys. Rev. A **51**, 4611 (1995).

GA89 J. O. Gaardsted and T. Andersen, J. Phys. B **22**, L51 (1989).

Gd99 R. J. Gdanitz, J. Chem. Phys. **110**, 706 (1999).

GDL93 N. D. Gibson, B. J. Davies, and D. J. Larson, Phys. Rev. A **47**, 1946 (1993).

GR88 C. H. Greene and N. Rouze, Z. Phys. D **9**, 219 (1988).

GWW89 Y. Guo, M. C. Wrinn, and M. A. Whitehead, Phys. Rev. A **40**, 6685 (1989).

HAA92 H. K. Haugen, L. H. Andersen, T. Andersen, P. Balling, N. Hertel, P. Hvelplund, and S. P.

Møller, Phys. Rev. A **46**, R1 (1992).
HC95 J.-J. Hsu and K. T. Chung, Phys. Rev. A **52**, R898 (1995).
HD96 S. Hati and D. Datta, J. Phys. Chem. **100**, 4828 (1996).
HG92 D. Hanstorp and M. Gustafsson, J. Phys. B **25**, 1773 (1992).
HHK96 G. Haeffler, D. Hanstorp, I. Kiyan, A. E. Klinkmüller, U. Ljungblad, and D. J. Pegg, Phys. Rev. A **53**, 4127 (1996).
HKR89 H. Haberland, T. Kolar, and T. Reiners, Phys. Rev. Lett. **63**, 1219 (1989).
HKR96 G. Haeffler, A. E. Klinkmüller, J. Rangell, U. Berzinsh, and D. Hanstorp, Z. Phys. D **38**, 211 (1996).
HL73 H. Hotop and W. C. Lineberger, J. Chem. Phys. **58**, 2379 (1973).
HL75 H. Hotop and W. C. Lineberger, J. Phys. Chem. Ref. Data **4**, 539 (1975).
HL85 H. Hotop and W. C. Lineberger, J. Phys. Chem. Ref. Data **14**, 731 (1985).
HLH93 H. W. van der Hart, C. Laughlin, and J. E. Hansen, Phys. Rev. Lett. **71**, 1506 (1993).
HLK97 G. Haeffler, U. Ljungblad, I. Yu. Kiyan, and D. Hanstorp, Z. Phys. D **42**, 263 (1997).
Ho98 H. Hotop (unpublished, 1998).
HPL73 H. Hotop, T. A. Patterson, and W. C. Lineberger, Phys. Rev. A **8**, 762 (1973).
HRB65 J. L. Hall, E. J. Robinson, and L. M. Branscomb, Phys. Rev. Lett. **14**, 1013 (1965).
HZG97 O. Harms, M. Zehnpfennig, V. Gomer, and D. Meschede, J. Phys. B **30**, 3781 (1997).
ISS87 R. N. Ilin, V. I. Sakharov, and I. T. Serenkov, Opt. Spectrosc. (USSR) **62**, 578 (1987) [Opt. Spektrosk. **62**, 976 (1987)].
JBB85 P. Juncar, C. R. Bingham, J. A. Bounds, D. J. Pegg, H. K. Carter, R. L. Mlekodaj, and J. D. Cole, Phys. Rev. Lett. **54**, 11 (1985).
KAC85 T. J. Kvale, G. D. Alton, R. N. Compton, D. J. Pegg, and J. S. Thompson, Phys. Rev. Lett. **55**, 484 (1985).
KBA99 L. Knoll, K. G. Bhushan, N. Altstein, D. Zajfman, O. Heber, and M. L. Rappaport, Phys. Rev. A **60**, 1710 (1999).
KBP97 P. Kristensen, C. A. Brodie, U. V. Pedersen, V. V. Petrunin, and T. Andersen, Phys. Rev. Lett. **78**, 2329 (1997).
KHL75 A. Kasdan, E. Herbst, and W. C. Lineberger, J. Chem. Phys. **62**, 541 (1975).
KPA95 P. Kristensen, V. V. Petrunin, H. H. Andersen, and T. Andersen, Phys. Rev. A **52**, R2508 (1995).
KPP97 P. Kristensen, U. V. Pedersen, V. V. Petrunin, T. Andersen, and K. T. Chung, Phys. Rev. A **55**, 978 (1997).
KPR85 M. Kaivola, O. Poulsen, E. Riis, and S. A. Lee, Phys. Rev. Lett. **54**, 255 (1985).
KR83 P. Kruit and F. H. Read, J. Phys. E **16**, 31 (1983).
KSB93 P. Kristensen, H. Stapelfeldt, P. Balling, T Andersen, and H. K. Haugen, Phys. Rev. Let **71**, 3435 (1993).
LKG91 A. E. Litherland, L. R. Kilius, M. A. Garwar M.-J. Nadeau, and X.-L. Zhao, J. Phys. B **2** L233 (1991).
LL86 D. G. Leopold and W. C. Lineberger, J. Chen Phys. **85**, 51 (1986).
LML91 K. R. Lykke, K. K. Murray, and W. C Lineberger, Phys. Rev. A **43**, 6104 (1991).
LS85 D. J. Larson and R. Stoneman, Phys. Rev. A **3** 2210 (1985).
LXL98 T. P. Lippa, S.-J. Xu, S. A. Lyapustina, J. M Nilles, and K. H. Bowen, J. Chem. Phys. **10** 10727 (1998).
Ma65 T. F. O'Malley, Phys. Rev. **137**, A1668 (1965)
MAK80 S. Mannervik, G. Astner, and M. Kisielinski, Phys. B **13**, L441 (1980).
MEL88 N. B. Mansour, C. J. Edge, and D. J. Larson Nucl. Instrum. Methods Phys. Res. B **31**, 3 (1988).
MGH78 J. Mazeau, F. Gresteau, R. I. Hall, and A. Huet J. Phys. B **11**, L557 (1978).
Mi83 R. Middleton, Nucl. Instrum. Methods. **214**, 13 (1983).
Mi89 R. Middleton, *A Negative-Ion Cookbook* (Un versity of Pennsylvania Press, Philadelphia, P 1989).
MLL84 R. D. Mead, K. R. Lykke, W. C. Lineberger, Marks, and J. I. Brauman, J. Chem. Phys. **8** 4883 (1984).
MN73 D. L. Mader and R. Novick, *Atomic Physics* (Plenum, New York, 1973), p. 169.
MSL86 T. M. Miller, A. E. Stevens Miller, and W. C Lineberger, Phys. Rev. A **33**, 3558 (1986).
NA91 C. A. Nicolaides and G. Aspromallis, Phys. Re A **44**, 2217 (1991).
NBB99 P. L. Norquist, D. R. Beck, R. C. Bilodeau, M Scheer, R. A. Srawley, and H. K. Haugen, Phy Rev. A **59**, 1896 (1999).
NGZ97 M-J. Nadeau, M. A. Garwan, X-L. Zhao, and A E. Litherland, Nucl. Instrum. Methods Phys. Re B **123**, 521 (1997).
NLA85 D. M. Neumark, K. R. Lykke, T. Andersen, an W. C. Lineberger, Phys. Rev. A **32**, 1890 (1985
NZG92 M.-J. Nadeau, X.-L. Zhao, M. A. Garwan, an A. E. Litherland, Phys. Rev. A **46**, R358 (1992).
NW70 R. Novick and D. Weinflash, in *Proceedings the International Conference on Precision an Fundamental Constants*, Nat. Bur. Stand. (US Spec. Publ. No 343, edited by D. N. Langenber and N. N. Taylor (U. S. GPO, Washington, DC 1970), p. 403.

OPS94 J. Olsen, L. G. M. Pettersson, and D. Sundholm, J. Phys. B **27**, 5575 (1994).

PAA98 U. V. Pedersen, H. H. Andersen, T. Andersen, and L. Veseth, Phys. Rev. A **58**, 258 (1998).

PAB96 V. V. Petrunin, H. H. Andersen, P. Balling, and T. Andersen, Phys. Rev. Lett. **76**, 744 (1996).

PBK98 V. V. Petrunin, C. A. Brodie, P. Kristensen, U. V. Pedersen, and T. Andersen, J. Phys. B **31**, L415 (1998).

Pe62 C. L. Pekeris, Phys. Rev. **126**, 1470 (1962).

Pe92 J. R. Peterson, Aust. J. Phys. **45**, 293 (1992).

PTC87 D. J. Pegg, J. S. Thompson, R. N. Compton, and G. D. Alton, Phys. Rev. Lett. **59**, 2267 (1987).

PVB95 V. V. Petrunin, J. D. Voldstad, P. Balling, P. Kristensen, T. Andersen, and H. K. Haugen, Phys. Rev. Lett. **75**, 1911 (1995).

RRH98 M. Reicherts, M.-W. Ruf, and H. Hotop (private communication, 1998).

SBB91 H. Stapelfeldt, P. Balling, C. Brink, and H. K. Haugen, Phys. Rev. Lett. **67**, 1731 (1991).

SBB98a M. Scheer, C. A. Brodie, R. C. Bilodeau, and H. K. Haugen, Phys. Rev. A **58**, 2051 (1998).

SBB98b M. Scheer, R. C. Bilodeau, C. A. Brodie, and H. K. Haugen, Phys. Rev. A **58**, 2844 (1998).

SBG71 F. R. Simpson, R. Browning, and H. B. Gilbody, J. Phys. **4**, 106 (1971).

SBH98a M. Scheer, R. C. Bilodeau, and H. K. Haugen, J. Phys. B **31**, L11 (1998).

SBH98b M. Scheer, R. C. Bilodeau, and H. K. Haugen, Phys. Rev. Lett. **80**, 2562 (1998).

SBT98 M. Scheer, R. C. Bilodeau, J. Thøgersen, and H. K. Haugen, Phys. Rev. A **57**, R1493 (1998).

Sc98 M. Scheer, PhD thesis, McMaster University, Hamilton, Canada, 1998.

Sh97 V. P. Shevelko, *Atoms and Their Spectroscopic Properties*, Springer Series on Atoms and Plasmas, Vol 18 (Springer, Berlin, 1997).

SHB97 M. Scheer, H. K. Haugen, and D. R. Beck, Phys. Rev. Lett. **79**, 4104 (1997).

SL77 J. Slater and W. C. Lineberger, Phys. Rev. A **15**, 2277 (1977).

SML85 P. A. Schulz, R. D. Mead, and W. C. Lineberger (private communication, 1985).

SRN78 J. Slater, F. H. Read, S. E. Novick, and W. C. Lineberger, Phys. Rev. A **17**, 201 (1978).

STB98 M. Scheer, J. Thøgersen, R. C. Bilodeau, C. A. Brodie, H. K. Haugen, H. H. Andersen, P. Kristensen, and T. Andersen, Phys. Rev. Lett. **80**, 684 (1998).

SW79 R. M. Stehman and S. B. Woo, Phys. Rev. A **20**, 281 (1979).

SWL96 S. Salomonson, H. Warston, and I. Lindgren, Phys. Rev. Lett. **76**, 3092 (1996).

Ta99 B. N. Taylor (private communication, 1999).

TSS96a J. Thøgersen, L. D. Steele, M. Scheer, H. K. Haugen, P. Kristensen, P. Balling, H. Stapelfeldt, and T. Andersen, Phys. Rev. A **53**, 3023 (1996).

TSS96b J. Thøgersen, L. D. Steele, M. Scheer, C. A. Brodie, and H. K. Haugen, J. Phys. B **29**, 1323 (1996).

TSS96c J. Thøgersen, M. Scheer, L. D. Steele, H. K. Haugen, and W. P. Wijesundera, Phys. Rev. Lett. **76**, 2870 (1996).

TWP93 C. Y. Tang, J. R. Wood, D. J. Pegg, J. Dellwo, and G. D. Alton, Phys. Rev. A **48**, 1983 (1993).

VBD99 C. Valli, C. Blondel, and C. Delsart, Phys. Rev. A **59**, 3809 (1999).

VC93 S. H. Vosko and J. A. Chevary, J. Phys. B **26**, 873 (1993).

VDH98 I. Velchev, R. van Dierendonck, W. Hogervorst, and W. Ubachs, J. Mol. Spectrosc. **187**, 21 (1998).

VLM89 S. H. Vosko, J. B. Lagowski, and I. L. Mayer, Phys. Rev. A **39** 446 (1989).

WBB99 A. Wolf, K. G. Bhushan, I. Ben-Itzhak, N. Altstein, D. Zajfman, O. Heber, and M. L. Rappaport, Phys. Rev. A **59**, 267 (1999).

WCC98a W. W. Williams, D. L. Carpenter, A. M. Covington, M. C. Koepnick, D. Calabrese, and J. S. Thompson, J. Phys. B **31**, L341 (1998).

WCC98b W. W. Williams, D. L. Carpenter, A. M. Covington, J. S. Thompson, T. J. Kvale, and D. G. Seely, Phys. Rev. A **58**, 3582 (1998).

Wi48 E. P. Wigner, Phys. Rev. **73**, 1002 (1948).

Wi97 W. P. Wijesundera, Phys. Rev. A **55**, 1785 (1997).

WP92 C. W. Walter and J. R. Peterson, Phys. Rev. Lett. **68**, 2281 (1992).

YC99 Z. C. Yan and K. T. Chung (private communication, 1999).

ZNG93 X-L. Zhao, M. J. Nadeau, M. A. Garwan, L. R. Kilius, and A. E. Litherland, Phys. Rev. A **48**, 3980 (1993).